



HAL
open science

Strontium isotope evidence for Pre-Islamic cotton cultivation in Arabia

Saskia E Ryan, Éric Douville, Arnaud Dapoigny, Pierre Deschamps, Vincent Battesti, Abel Guihou, Matthieu Lebon, Jérôme Rohmer, Vladimir Dabrowski, Patricia Dal Prà, et al.

► **To cite this version:**

Saskia E Ryan, Éric Douville, Arnaud Dapoigny, Pierre Deschamps, Vincent Battesti, et al.. Strontium isotope evidence for Pre-Islamic cotton cultivation in Arabia. *Frontiers in Earth Science*, 2023, 11, pp.1257482. 10.3389/feart.2023.1257482 . mnhn-04351509

HAL Id: mnhn-04351509

<https://mnhn.hal.science/mnhn-04351509>

Submitted on 21 Dec 2023

HAL is a multi-disciplinary open access archive for the deposit and dissemination of scientific research documents, whether they are published or not. The documents may come from teaching and research institutions in France or abroad, or from public or private research centers.

L'archive ouverte pluridisciplinaire **HAL**, est destinée au dépôt et à la diffusion de documents scientifiques de niveau recherche, publiés ou non, émanant des établissements d'enseignement et de recherche français ou étrangers, des laboratoires publics ou privés.



Distributed under a Creative Commons Attribution - NonCommercial - NoDerivatives 4.0 International License



OPEN ACCESS

EDITED BY

Dominik Fleitmann,
University of Basel, Switzerland

REVIEWED BY

Yehudit Harlavan,
Geological Survey of Israel, Israel
Nadia Solovieva,
University College London,
United Kingdom

*CORRESPONDENCE

Saskia E. Ryan,
✉ ryans22@tcd.ie

[†]These authors have contributed equally
to this work

RECEIVED 20 July 2023

ACCEPTED 07 November 2023

PUBLISHED 18 December 2023

CITATION

Ryan SE, Douville E, Dapoigny A,
Deschamps P, Battesti V, Guihou A,
Lebon M, Rohmer J, Dabrowski V,
Dal Prà P, Nehmé L, Zazzo A and
Bouchaud C (2023), Strontium isotope
evidence for Pre-Islamic cotton
cultivation in Arabia.
Front. Earth Sci. 11:1257482.
doi: 10.3389/feart.2023.1257482

COPYRIGHT

© 2023 Ryan, Douville, Dapoigny,
Deschamps, Battesti, Guihou, Lebon,
Rohmer, Dabrowski, Dal Prà, Nehmé,
Zazzo and Bouchaud. This is an open-
access article distributed under the terms
of the [Creative Commons Attribution
License \(CC BY\)](https://creativecommons.org/licenses/by/4.0/). The use, distribution or
reproduction in other forums is
permitted, provided the original author(s)
and the copyright owner(s) are credited
and that the original publication in this
journal is cited, in accordance with
accepted academic practice. No use,
distribution or reproduction is permitted
which does not comply with these terms.

Strontium isotope evidence for Pre-Islamic cotton cultivation in Arabia

Saskia E. Ryan^{1,2*}, Eric Douville², Arnaud Dapoigny²,
Pierre Deschamps³, Vincent Battesti⁴, Abel Guihou³,
Matthieu Lebon⁵, Jérôme Rohmer⁶, Vladimir Dabrowski¹,
Patricia Dal Prà⁷, Laïla Nehmé⁸, Antoine Zazzo^{1†} and
Charlène Bouchaud^{1†}

¹Archéozoologie, Archéobotanique: Sociétés, Pratiques et Environnements (AASPE, UMR 7209), Muséum National d'Histoire Naturelle, CNRS, Paris, France, ²Laboratoire des Sciences du Climat et de l'Environnement, LSCE/IPSL, UMR CEA-CNRS-UVSQ, Université Paris-Saclay, Gif-sur-Yvette, France, ³Aix Marseille University, CNRS, IRD, INRAE, CEREGE, Aix-en-Provence, France, ⁴Éco-Anthropologie (EA UMR 7206), CNRS, Muséum National d'Histoire Naturelle, Université Paris Cité, Musée de l'Homme, Paris, France, ⁵Histoire Naturelle de l'Homme Préhistorique (HNHP, UMR 7194), Muséum National d'Histoire Naturelle, CNRS, UPVD, Musée de l'Homme, Paris, France, ⁶CNRS, UMR 8167 Orient & Méditerranée, Ivry-sur-Seine, France, ⁷Institut National du Patrimoine, Aubervilliers, France, ⁸Orient & Méditerranée (UMR 8167), CNRS, Ivry-sur-Seine, France

With a view to understanding the dynamics of ancient trade and agrobiodiversity, archaeobotanical remains provide a means of tracing the trajectories of certain agricultural commodities. A prime example is cotton in Arabia, a plant that is non-native but has been found in raw seed and processed textile form at Hegra and Dadan, in the region of al-‘Ulā, north-western Saudi Arabia—sites of critical importance given their role in the trans-Arabian trading routes during Antiquity. Here, we demonstrate that the measurement of strontium isotopes from pre-cleaned archaeological cotton is methodologically sound and is an informative addition to the study of ancient plant/textile provenance, in this case, putting forward evidence for local production of cotton in oasis agrosystems and possible external supply. The presence of locally-grown cotton at these sites from the late 1st c. BCE—mid 6th c. CE is significant as it demonstrates that cotton cultivation in Arabia was a Pre-Islamic socio-technical feat, while imported cotton highlights the dynamism of trade at that time.

KEYWORDS

cotton (*Gossypium arboreum/herbaceum*), strontium isotopes, provenance, Nabatean Kingdom, Hegra, Dadan, Saudi Arabia, archaeobotany

1 Introduction

Reconstructing ancient plant provenance informs on past agricultural systems, economies and trade but comes with its challenges. These are due in some cases to poor and/or unrepresentative sources (or proxies), but often hindered by methodological barriers. A pertinent example of this is cotton (*Gossypium arboreum/herbaceum*, Malvaceae), a plant which was originally domesticated in tropical and sub-tropical zones of the Indian sub-continent (for *G. arboreum*) and Africa (for *G. herbaceum*) but has since reached extensive geographical coverage (Kulkarni et al., 2009; Viot, 2019). Its cultivation in the desert environment that exists over much of the Arabian Peninsula provides a case study to

understand past diffusion paths and trade dynamics of a non-native plant. It was long considered that this plant was introduced with the so-called “Arab agricultural revolution” (Watson, 1974). This concept, based on the study of written sources, suggests the 7th c. CE Islamic conquest and unification of the Middle East, Central Asia and Mediterranean regions created opportunities for acclimatization of new crops, including cotton (Watson, 1974; Watson, 1981; Watson, 1983). Watson’s thesis has been influential (Squatriti, 2014), although more recent works, especially archaeobotanical studies, have provided a more nuanced view by hypothesizing Pre-Islamic plant introduction (Decker, 2009; Bouchaud et al., 2011; Bouchaud, 2015; Bouchaud et al., 2018; Fuks et al., 2020). In this paper, we aim to use the strontium (Sr) isotope composition of cotton in order to determine if 1) there was local production of cotton before the Islamic period in the northern part of the Arabian Peninsula, or 2) the material found on site was imported or 3) a combination of these two scenarios was taking place.

Cotton is non-native to the Arabian Peninsula, but archaeological and textual sources demonstrate that it has a long history in the region. To the North in the Levant, early traces of cotton fibers were found at Tel Tsaf, Israel (ca. 5200–4700 BCE) (Liu et al., 2022) and at Dhuweila, eastern Jordan (4450–3000 BCE) (Betts et al., 1994) suggesting possible very ancient trade of cotton fibers. The Greek philosopher and botanist Theophrastus (371–288 BCE) (*Historia Plantarum*, IV.7.7 [Amigues, 2010, p. 159]), mentions the cultivation of “wool-bearing trees” in Arabia for the first time during the 4th c. BCE on the island of Tylos, namely, the Bahrain archipelago. This textual reference, in conjunction with the north-western archaeological preserved cotton remains in the form of seeds, bolls (raw unginned fibers) and textiles in later sites such as Aila in southern Jordan (Ramsay and Parker, 2016), Hegra in northwestern Arabia (Bouchaud et al., 2018; Bouchaud et al., 2011) and Mleiha in the UAE (Kerfant and Dabrowski, 2017; Ryan et al., 2021), provide evidence for the far-reaching presence of cotton across the Arabian Peninsula by the turn of the 1st mill. CE. However, the simple occurrence alone of cotton does not prove that local cultivation of the crop was taking place. It remains difficult to demonstrate without ambiguity that the archaeological material testifies to the introduction of cotton agriculture rather than to the importation of cotton products by long-distance trade. At the site of Mleiha (Sharjah, United Arab Emirates), for instance, both charred cotton seeds and textiles were found in a burned-down building, radiocarbon dated to the beginning of the 3rd c. CE (Ryan et al., 2021). The strontium isotope values of archaeological cotton from Mleiha were inconsistent with those observed from modern plants growing both in the immediate vicinity of the site and in the region surrounding it and they are therefore considered as “non-local” (Ryan et al., 2021). The relatively radiogenic, non-local cotton remains were likely sourced from vast distances away, with strontium isotope data, archaeological and textual evidence pointing towards regions of western India as the likely place of origin.

Some of the first direct archaeological evidence of cotton in the Arabian Peninsula comes from the two sites that are the subject of this study: Hegra/Mada’in Sālih, today al-Hijr (26°47′ 1.38″ N; 37° 57′ 16.81″ E) and Dadan/al-Khurybah (26° 39′ 23.3″ N; 37° 54′ 57.31″ E), both located in north-west Saudi Arabia in the al-‘Ulā region (Supplementary Appendix S1). Hundreds of carbonized cotton seeds were unearthed suggesting that cotton bolls were

being processed, i.e., the fibers were removed from the seeds in the domestic areas, making it very plausible for cotton to have been grown locally over centuries (Bouchaud et al., 2011; Bouchaud et al., 2018; Charloux et al., 2018). However, the provenance of the seeds is ambiguous and it is even less certain whether desiccated textiles, uncovered within funerary chambers at Hegra, were produced locally or imported.

In the current paper, we aim to use strontium isotope ratios of both the archaeological charred cotton seeds and the desiccated textiles to determine if they were out-sourced or potentially produced on site. To do so, comparison with modern bio-available reference material, including plants and groundwater, is used to understand what can be deemed as ‘local’ from a geochemical standpoint. Radiocarbon dating of the material is undertaken to establish the precise chronology of cotton spread into Arabia. Isotope data already obtained from other Late Pre-Islamic sites (Ryan et al., 2021) is also drawn on to define more clearly the nature and chronology of the cotton spread throughout the Arabian Peninsula.

The use of strontium isotopes as a provenance tool is underpinned by the fact that strontium from bedrock is assimilated by plants, thus plants retain the isotopic fingerprint of the geological setting in which they grew (Capo et al., 1998). This allows geological and consequently, geographical variation in the radiogenic Sr isotope values (reported as the isotope ratio $^{87}\text{Sr}/^{86}\text{Sr}$) of plant materials to be matched with, or distinguished from, a local site geology. Strontium isotopes have previously been used in an attempt to provenance plant material, such as wooden timbers (English et al., 2001; Reynolds et al., 2005; Hajj et al., 2017; Domínguez-Delmás et al., 2020; Pinta et al., 2021), textiles including cotton (Frei and Bjerregaard, 2017; Stanish et al., 2018; Ryan et al., 2021; Wozniak and Belka, 2022) and willow and tulle (Benson et al., 2006). In a recent isotopic study of ancient cotton textiles, Wozniak and Belka (2022) suggest that Late Antique and Medieval cotton fabrics found in the middle of the Nile Valley (Sudan) could not have been grown locally based on their too-radiogenic strontium isotope values and technical characteristics, instead linking their presence to trade from potential places including Western Egypt, the west coast of India, Pakistan or the Arabian Peninsula. This study, as well as the aforementioned study conducted on cotton seeds and textiles at Mleiha, Eastern Arabia (Ryan et al., 2021), attest to the ancient long-distance, transcontinental trade of cotton. Such isotopic investigations into archaeological plant and textile origins are still relatively rare due to concerns over potential contamination with Sr from the burial environment. It is well established that some plant material, such as timber, is highly susceptible to diagenetic alteration from waterlogging in the burial environment (Van Ham-Meert et al., 2020; Snoeck et al., 2021). While water saturation is not considered an issue here, given the arid environmental conditions that resulted in the desiccation of the textiles and the charred state of the seeds that enabled their exceptional conservation, sand and dust contaminants are of concern. It has been demonstrated that leachates and residual cotton material differ in their $^{87}\text{Sr}/^{86}\text{Sr}$ ratios (Ryan et al., 2021), indicating the existence of exogenous Sr adhering to the archaeological remains, which could potentially complicate the interpretation of Sr isotope signature of botanical material. In the case of animal-derived textile material, a number of

studies have shown that while desiccated wool textiles can adsorb exogenous Sr from the soil in which they are buried, it is possible to remove, at least in part, contaminant Sr by leaching the textile in acid, enabling one to determine if the strontium isotope value of residual material overlaps or not with the Sr isotope signature of the local area (Frei et al., 2009a; Frei et al., 2009b; Frei et al., 2010; Bergfjord et al., 2012; Frei et al., 2015; Frei et al., 2017). Here, we test an acid-leach protocol on cotton, linen and wool textiles and cotton seeds to ensure the methodology is appropriate for use when measuring the $^{87}\text{Sr}/^{86}\text{Sr}$ values on these materials and that it is possible to extract reliable provenance information from ancient plant materials.

2 Methods

2.1 Contaminant detection and removal

Residues were identified on the surfaces of the textiles. To identify the nature of these residues, a subset of six textiles were selected for Fourier transform infrared spectroscopy (FTIR) analysis (See [Supplementary Material](#) for full details). The analyses were carried out in transmission mode (after pressing the sample in a diamond cell), on the infrared spectroscopy platform of the Muséum national d'Histoire naturelle (MNHN, Paris).

Acid leaching was required to pre-clean the archaeological material (details in [Supplementary Appendix S3](#)). The resulting acid leachates and residual textiles were analyzed to test the efficacy of this pre-cleaning treatment. Four archaeological cotton textiles from the site of Mleiha and their corresponding acid leachates were previously analyzed for their strontium isotope composition (Ryan et al., 2021), and here, were analyzed for strontium concentrations. This material provides an external check on the efficacy of the pre-treatment.

2.2 Digestion and ion chromatographic procedures

The entire acid digestion process (Ryan et al., 2021) and subsequent Sr purification were achieved under a class 100 laminar flow hood in a class 10,000 clean room (ISO 7).

Strontium isotopic analyses of groundwater samples were carried out at the European Center for Research and Education in Environmental Geosciences (CEREGE, Aix-en-Provence, France) following a procedure described in Mahamat Nour et al. (2020). A volume of water corresponding to about 200 ng of Sr was evaporated. Separation and purification of the strontium fraction were carried out using the Sr-Spec resin on a 200 μL column in HNO_3 media. The fraction was evaporated and then attacked with $\text{HNO}_3 + \text{H}_2\text{O}_2$ to mineralize any organic residues of the Sr-Spec resin.

2.3 Mass spectrometry

Strontium isotope analyses of the botanical material were performed on a Thermo Scientific Neptune^{plus} Multi-Collector

Inductively Coupled Plasma Mass Spectrometer (MC-ICPMS), at the Laboratoire des Sciences du Climat et de l'Environnement (LSCE, France). The purified strontium fractions were adjusted to a strontium concentration of 20 $\mu\text{g}/\text{L}$ by dilution with 0.5 N HNO_3 . The LSCE has recently updated the analytical method for measurement of Sr isotopes using MC-ICPMS—for details see Ryan et al. (2021).

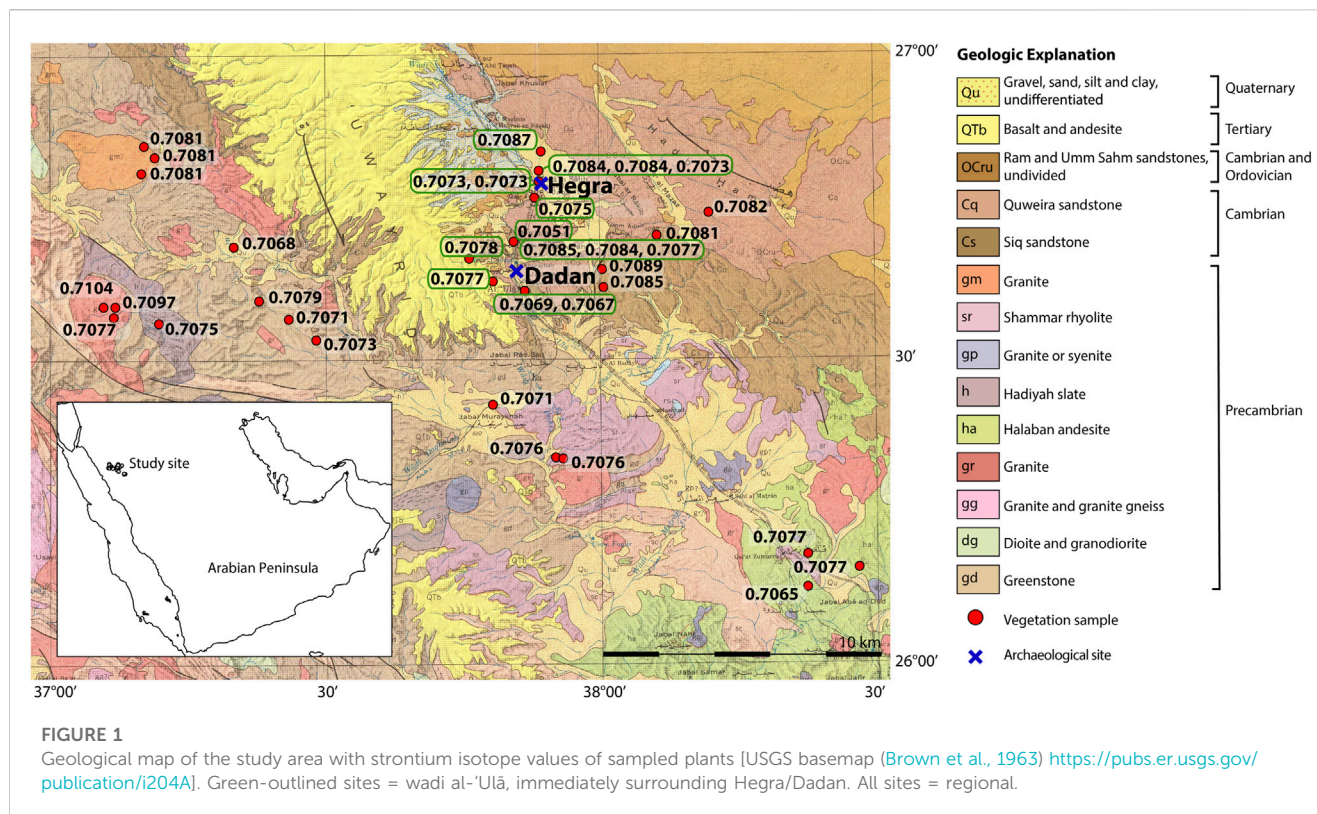
The reproducibility of the $^{87}\text{Sr}/^{86}\text{Sr}$ measurements was evaluated by repeated analysis of NBS 987 standard. Mean values of 0.710231 ± 0.000005 ($n = 27$), 0.710265 ± 0.000008 ($n = 35$) and 0.710281 ± 0.000007 ($n = 35$) were obtained in this study across three runs. Isotopic ratios were corrected using a standard-sample bracketing method and normalized to the NBS 987 standard value of 0.710245. The corresponding external reproducibility measured for the 3 runs using NBS 987 standard ranged between 14 and 22 ppm (2σ). For each sample, the $^{87}\text{Sr}/^{86}\text{Sr}$ value is reported with a 2σ uncertainty, taking into account the standard reproducibility and the measurement standard error of each sample. However, such analytical precision does not take into account the uncertainties related to the efficiency of the different treatments applied to the samples, their size or the Sr content present in the remains after leaching or the fact that it is difficult to perform meaningful reproducibility tests on such small samples. For this reason, in this study, we considered the values of Sr isotope ratios to the fourth decimal place.

For groundwater samples, strontium isotopes were performed on a Neptune^{plus} MC-ICP-MS at CEREGE. Dry samples were taken up and dissolved with HNO_3 1%. Long-term external reproducibility assessed through repeated analyses of the AQUA-1 drinking water certified reference material (Yeghicheyan et al., 2021) is better than 15 ppm.

2.4 Radiocarbon dating

Five cotton seeds and two pieces of cotton textile were selected from different contexts at Hegra. In addition, two seeds of date palm, one barley grain and two undetermined wood charcoal fragments uncovered in different archaeological units which also contained cotton seeds (but not a sufficient quantity for analysis) were selected. Two cotton seeds were selected from the site of Dadan. Eight of the samples were prepared at the ^{14}C lab of the MNHN and graphitization and ^{14}C measurements were carried out at LSCE (France) using the AGE 3 automatized graphitization system and the compact AMS ECHO MICADAS[®]. Six of the samples were prepared at the Centre de Datation par le Radio-Carbone in Lyon (France), combusted in a vacuum line and ca. 1 mg C of purified CO_2 was sealed in a glass tube, followed by graphitization with ^{14}C measurements being carried out on the ARTEMIS AMS in Saclay. In both cases, the materials were prepared for radiocarbon dating using the standard acid-alkali-acid (AAA) method.

The textile samples were prepared by addition of chloroform: methanol 2:1 followed by the classical AAA procedure: 1 N HCl for 1 h, 0.1 N NaOH at room temperature for 15 min, and again 1 N HCl for 30 min. They were then loaded into tin capsules prior to combustion and graphitized using an automated AGE 3 device. The radiocarbon ages were calibrated using the Oxcal 4.4. software and the IntCal20 atmospheric curve (Bronk Ramsey, 2020; Reimer et al., 2020).



2.5 ICP-MS determination of trace elements

Strontium concentrations were measured via the LSCE's Inductively Coupled Plasma Mass Spectrometry Thermo Scientific iCAP TQ. In preparation for analysis, a 0.2 mL aliquot of each of the solutions was sub-sampled and diluted to produce a 2% (v/v) HNO₃ solution bearing a mixed internal standard with Ge, In and Re for the purpose of correcting instrument drift and signal suppression during analysis. To evaluate analytical uncertainties linked to Sr concentration measurements, two geo-standards, USGS BCR-1 (basalt) and NIST SRM 1640a (water), were regularly analyzed during the Q ICP-MS run. The measured mean values were $1,401 \pm 97$ mg/kg ($n = 5$) and 129 ± 5 μg/L, respectively in agreement with expected reference values and with an analytical uncertainty of 7% and 4% (1 σ), respectively.

3 Results

3.1 Modern plants

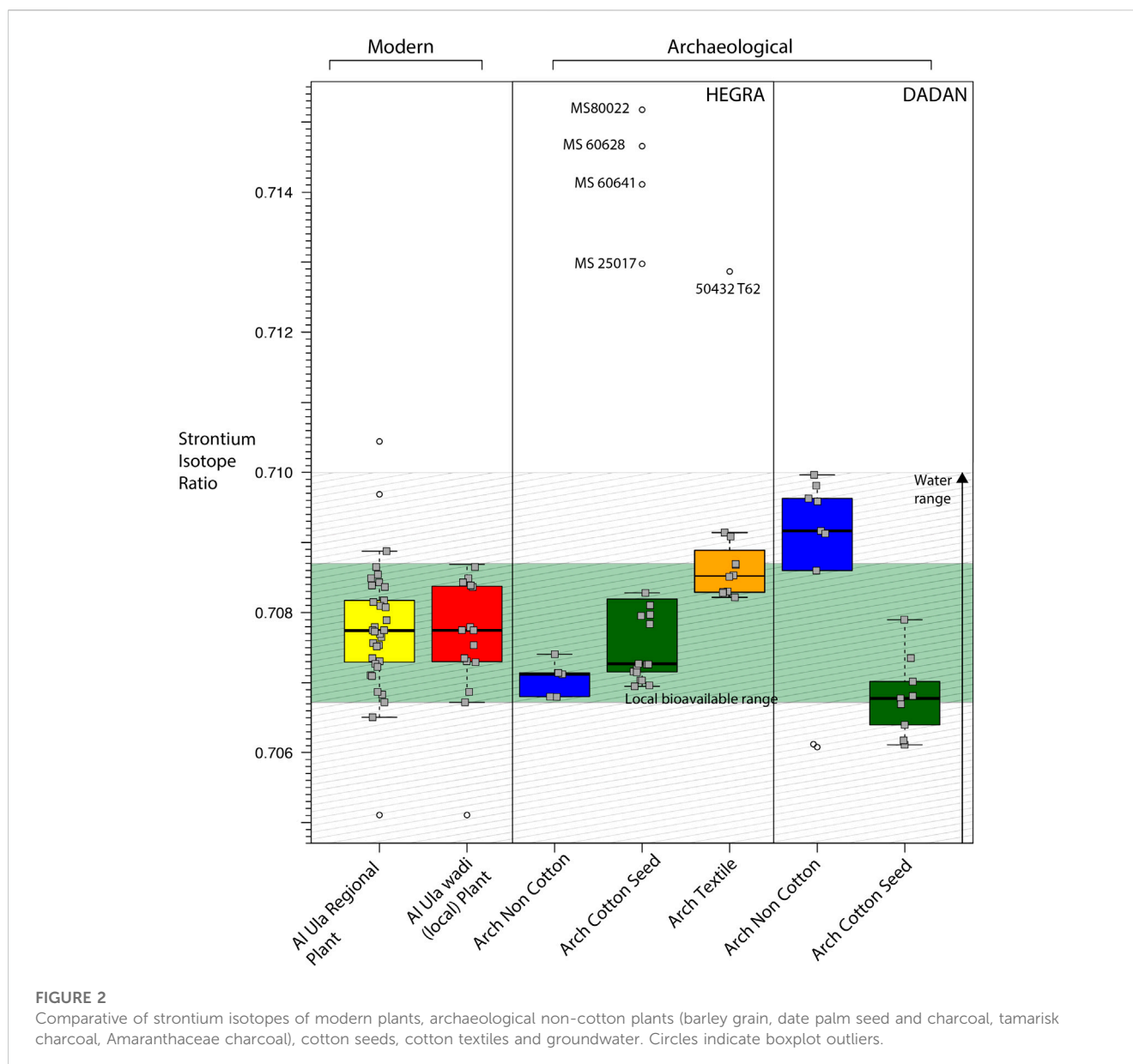
Fifteen modern plants collected from the wadi al-Ulā, and twenty-two modern plant samples from the wider region were analyzed to characterize ⁸⁷Sr/⁸⁶Sr variations across the region (Figures 1, 2). ⁸⁷Sr/⁸⁶Sr values of all plants from the entire region ranged from 0.7051 to 0.7104 ($n = 37$) (Supplementary Table S1). These data define what can be considered as the regional range in bioavailable strontium values (see open and closed circles in Figure 3).

⁸⁷Sr/⁸⁶Sr values of plants collected from the wadi al-Ulā ranged from 0.7051 to 0.7087 ($n = 15$), or 0.7067 to 0.7087 excluding one

outlier. The wadi broadly encompasses three geological groups. The Harrat al-Rahah and Harrat al-Uwayrid (QTb, Figure 1) are exposed directly north-west and west, respectively, of Hegra/Dadan and have a defined bio-available strontium isotope ratio of 0.7077 and 0.7078. Plants growing on the Cambrian Quweira (Cq) and Siq (Cs) sandstone outcrops directly at, and to the east of, Hegra/Dadan having values at 0.7075 and 0.7051, respectively. The modern plants overlying the Quaternary sediments in the low-lying region between the basalt and sandstone outcrops range from 0.7067 to 0.7087 ($n = 11$). These data define what can be considered as the local range in bioavailable strontium values (see open circles in Figure 3).

3.2 Groundwater

Analyses of strontium isotopes obtained on 71 groundwater samples collected in the Saq sandstone aquifer and alluvial aquifers located south of al-Ulā valley show ⁸⁷Sr/⁸⁶Sr values ranging between 0.7035 and 0.7099 (Figure 2; Supplementary Figure S2; Supplementary Table S2). Detailed study of major element analyses, together with a view to the spatial distribution of groundwater ⁸⁷Sr/⁸⁶Sr signature, show that this quite large range can be explained by the presence of two end-members contributing to the regional groundwater strontium composition (Deschamps et al., in prep): on one hand, a less radiogenic end-member (~0.704), consistent with the isotopic signature of the Harrat al-Uwayrid volcanic field that shows quite a homogeneous ⁸⁷Sr/⁸⁶Sr isotopic signature around 0.703 (Altherr et al., 2019; Sanfilippo et al., 2021), and, on the other hand, a more radiogenic end-member (~0.709) corresponding to



the fingerprint of the Saq sandstone end-member. Intermediate mixing between these two end-members is noted.

3.3 Archaeological material

The strontium isotope composition of 38 archaeological remains from Hegra and 18 from Dadan were analyzed (for sample details see [Supplementary Appendix S1](#)). This included seeds of cotton, textiles of cotton, linen and wool, seeds of date palm and barley, as well as tamarisk, date palm and Amaranthaceae charcoal. Date palm, barley and tamarisk at Hegra were found to range from 0.7068 to 0.7074 ($n = 5$) and those at Dadan from 0.7061 to 0.7100 ($n = 9$). FTIR analysis on a subset of the textiles from Hegra revealed the presence of non-cellulose material(s) on some of the fabrics ([Supplementary Appendix S2](#), [Supplementary Figures S3–S10](#), [Supplementary Table S3](#)), so acid leaching was used as an

effective pre-cleaning step to decontaminate the textiles ([Supplementary Appendix S3](#); [Supplementary Figure S11](#); [Supplementary Table S4](#)).

At Hegra, nineteen archaeological cotton seeds and twelve archaeological textiles (with two duplicates), ten of which are composed of cotton fibers, were analyzed. The isotopic range of the textiles composed only of cotton is 0.7082–0.7088. Duplicate cotton textiles measurements produce differences of Δ 0.000258 and 0.000033 from 50432_T41 and 50045_T06, respectively. This shows that heterogeneities in the textile strontium isotope values from a single fabric negate provenance interpretation on values on the order of the fourth decimal place or smaller. Archaeological wool textiles have much more disparate values (50240_T11 = 0.7092, 50240_L2 = 0.7087, 50432_T62 = 0.7129) and a textile with linen/cotton mixed composition had a value of 0.7091 (50432_T51). Excluding statistical outliers, archaeological cotton seeds range from

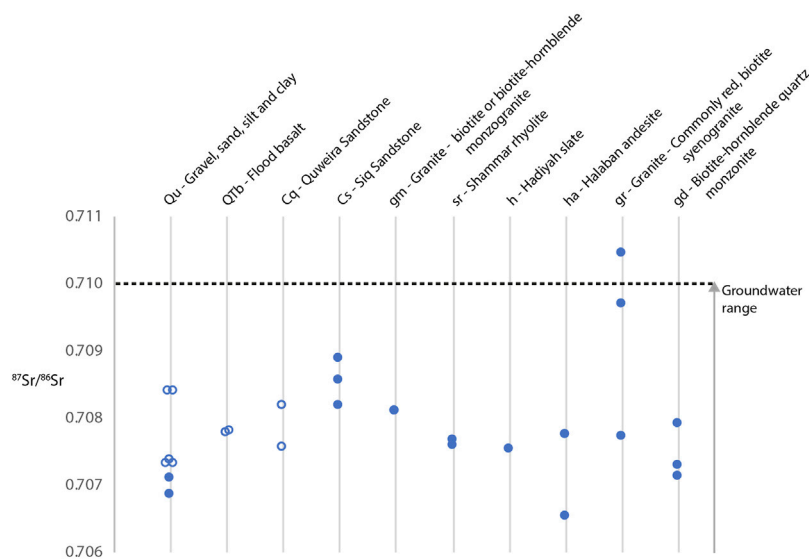


FIGURE 3

Strontium isotope values of modern bioavailable plant material, categorized based on the geological unit on which they grew. Open circles = local (Site of Hegra/Dadan and wadi al-'Ulā), all circles = regional.

0.7069 to 0.7083 ($n = 15$). At Dadan, nine archaeological cotton seeds range from 0.7061 to 0.7079 ($n = 9$).

3.4 Radiocarbon dates

The calibrated radiocarbon ages of the cotton textiles from Hegra range between 47 cal. BCE to 237 cal. CE (Supplementary Figure S12; Supplementary Table S5). Hegra cotton seeds date to a range from 120 cal. BCE to 423 cal. CE and those from Dadan date to a range from 415 to 547 cal. CE. From Hegra, a barley caryopsis, two date palm seeds and two undetermined charcoal fragments located in five stratigraphic units containing cotton seeds have a range in age from cal. 80 BCE to 540 cal. CE.

4 Discussion

4.1 Bioavailable (plant and water) strontium isotope values

Using both modern plants and waters is the gold standard when defining a regional baseline range in strontium isotope values, as has been done here for the extended al-'Ulā area. The collected plant samples cover a wide variety of geological bedrocks including basalt, granite, sandstone and sediments, ranging from Precambrian to Quaternary in age and have a range in strontium isotope values from 0.7051 to 0.7105 ($n = 37$) (Figure 2). While this range in the local and regional signatures is not geographically unique to this area, archaeological material with values falling widely outside this range signify material that is unlikely to have been grown within the region.

4.1.1 Modern, local plant signatures

Narrowing the geographical extent of the possible growth area correspondingly narrows the range in strontium isotope values one can deem as “local,” based on plant material alone. The Harrat al-Rahah and the Harrat al-'Uwayrid (QTb, Figure 1), the Cambrian Quweira sandstone outcrops to the east of Hegra (Cq) and plants overlying the Quaternary sediments (Qu) in the low-lying wadi al-'Ulā region between the basalt and sandstone outcrops range from 0.7067 to 0.7087 ($n = 14$, excludes one outlier). This range can be used as an upper and lower limit of what could be expected for plants growing locally (Figure 2), ideally to be considered in conjunction with the local water values.

4.1.2 Modern, regional groundwater signatures

While soil/regolith is the principal source of bioavailable strontium to plants, groundwater can have a critical effect on the isotopic composition of bioavailable strontium (Price et al., 2002; Bentley, 2006), especially in the case of oases where water input can be sizable. Moreover, soils average strontium over a relatively small area but ground/surface water generally average bioavailable strontium over a wider, regional catchment area (Evans et al., 2010; Willmes et al., 2014). Strontium isotope analyses of spring and well water from the al-'Ulā region illustrate that there are two clear end-members contributing to the regional water strontium composition. These water strontium isotope values encompass and surpass the entire range in bioavailable plant values, which represent the mixing of the two water Sr sources to varying degrees, in addition to the localized soil contribution. Due to the specific geographical configuration of the al-'Ulā area, groundwater from the Saq aquifer fed the oasis ecosystem during the historical period and was at the near surface (<8 m) up until the 1950s, as testified by observation of numerous abandoned jet

pumps in the valley. This would have made water easily accessible during the last millennia (Courbon, 2008), as such, water input was an important contributor to the potential local plant strontium budget, especially in an oasis setting.

4.1.3 Reconstructing ancient bioavailable signatures

When comparing the archaeological plant data from the sites of Dadan and Hegra, the growth environment needs to be considered. Archaeological seeds of barley ($n = 1$), date palm ($n = 2$) and wood charcoal from the Amaranthaceae family ($n = 2$), from Hegra as well as tamarisk ($n = 7$) and date palm charcoal ($n = 2$) from Dadan can be used as an additional proxy for baseline bioavailable values. This is because they are assumed to have been grown locally based on phytogeographical data, their presence in large quantities and their common occurrence at sites in Arabia since the Bronze Age (Tengberg, 2012). However, the growth environment may give rise to some disparities between supposed “local” values. Archaeological tamarisk from the site of Dadan has a mean of 0.7092 ± 0.0009 2SD ($n = 7$), while date palm charcoal has a mean of 0.7061 ± 0.001 2SD ($n = 2$) (Figure 2). The local water encapsulates this range in values. Less radiogenic basaltic-influenced groundwater input to oases may explain the lower values in the oasis date palm and other plants that grew in the most irrigated soils. More radiogenic water input, associated with sandstone lithologies in the region, could explain the higher values in plants such as tamarisk that would have grown on the edge of the palm grove (possibly planted and used for wood and as a rustic wind-breaker) or further out spontaneously on the sandy plain. Although of low probability, we cannot fully rule out that tamarisk could have come from a neighboring place with higher strontium values relative to the oasis-grown plants. We recommend that both modern local plants and water, as well as assumed locally-grown archaeological material, be collected as the best medium for defining the local baseline strontium isotope values to ensure the entire source pool(s) of strontium are covered, particularly for oasis environments.

4.2 First geochemical evidence of ancient cotton cultivation in Arabia

Prior to our initial analyses, no strontium isotope analyses on archaeological material from north-western Arabia had been carried out to date. The analyses of archaeological cotton seeds from Hegra exhibit a range in values between 0.7069 and 0.7152 ($n = 19$) (Supplementary Table S1). The vast majority of the archaeological cotton seeds ($n = 15$, out of 19 total) fall within what has been determined to be the local range, using local modern plant values ($n = 15$). We can consider two major origins for the seeds at Hegra. The first is a local, less radiogenic group ranging from 0.7069 to 0.7083 ($n = 15$), while the second is a non-local, more radiogenic group ranging from 0.7130 to 0.7152 ($n = 4$) (Figure 2). Within the former grouping, there is potentially a subgrouping due to local heterogeneities in the growth environment(s). At Dadan, four of the nineteen cotton seeds fall below 0.7067, the defined lower limit of the bioavailable modern plant range, but are still considered to be within the local water ranges.

Sr isotope values from processed textiles from Hegra have an overlapping but smaller range of 0.7082–0.7129 ($n = 14$ including two duplicates), with one clear statistical outlier made of wool (50432 T62) that does not fit within the local band of plant/water isotope values (Figure 2). This could be indicative that this wool textile was non-local, thus imported. Alternatively, it may be that the keratin is more susceptible to alteration from environmental processes than cotton fibers (Hu et al., 2020). Six of the textiles fall marginally within the defined local bioavailable strontium range and therefore are in line with production on site (Figure 2). In terms of the textile preparation, FTIR revealed the presence of gum, egg yolk and possibly madder on some of the cotton textiles (for details see Supplementary Table S3; Supplementary Figures S3–S10). None of these substances are indicative of a particular provenance as their use cannot be considered unusual at this place or time. The presence of madder was already known in Hegra on wool textile (Bouchaud et al., 2015). From an archaeological perspective, certain properties of textiles can be used to distinguish different textile-producing spheres, namely, the way in which the threads have been spun, i.e., clockwise (Z) or anticlockwise (S) (Wild, 1997). This tends to have cultural and thus, geographical associations, however, this is a very limited approach which must be used as an indicator only in combination with other lines of evidence (Bouchaud et al., 2019). All of the cotton textiles from Hegra are Z-spun (Supplementary Table S3), potentially a style of the Nabatean textile industry (Bouchaud et al., 2011). Based on the isotope data and material evidence, local cotton textile production at Hegra is most probable; it also appears from the isotope data that a smaller proportion of the studied cotton seeds—likely in the form of raw cotton balls—were traded to the site of Hegra.

It cannot be entirely ruled out that the cotton material falling within the bioavailable local ranges defined here were grown elsewhere, in a region with overlapping bioavailable isotope values. For instance, strontium isotope analysis of human and faunal remains, as well as groundwater, from the port city of Aila, southern Jordan, demonstrate a local and immigrant population profile with local values 0.7076–0.7086 (Perry et al., 2017). Human dental enamel from Egyptian and Nubian sites have $^{87}\text{Sr}/^{86}\text{Sr}$ values in agreement with the local values to al-‘Ulā (mean of 0.7078 ± 0.0003 and 0.7076 ± 0.0004 , respectively, with faunal material from the Nile Valley having a mean of 0.7079 ± 0.0023 , $n = 61$) (Buzon and Simonetti, 2013) and $^{87}\text{Sr}/^{86}\text{Sr}$ values of 75 human dental enamel samples from Tell el-Dabca in Egypt have a mean of 0.7079 ± 0.0002 (Stantis et al., 2020). Wool textiles from the Nile Valley, with a range of 0.7075–0.7084, fall within the supposed local values for the region from which they were excavated based on sheep/goat values of 0.7068–0.7082 (Wozniak and Belka, 2022). Bioavailable strontium isotope values from modern plants from Egypt and the southern Levant have a mean of 0.7086 ± 0.0003 (Arnold et al., 2016). Further east, sites from Pakistan, Iran, Iraq, Kuwait, Bahrain and UAE have values within the “local” al-‘Ulā range (see Ryan et al., 2021 for a compilation of references therein). Despite the existence of these isotopically overlapping regions of potential origin, the cotton seeds from Hegra were found in the context of habitats, in domestic fireplaces and dumping areas, likely having been disposed of as part of the ginning process (Bouchaud et al., 2011; Bouchaud et al., 2018; Charloux et al., 2018). The context of the finds, combined with

the large quantity of seeds over centuries, again suggests local processing.

While modern plant material is used here to give a range of potential regional values across the varied geological units, in reality, cotton would have only been feasibly grown close enough to an irrigation system (see [Supplementary Figure S2](#) for location and distribution of archaeological wells at Madā'in Salih; the water structures at Dadan in the Late Antique period are as of yet unknown but under study) and within the agricultural plots dedicated to the other oasian palm grove crops ([Bouchaud et al., 2011](#); [Bouchaud et al., 2018](#)) probably located within or in the close vicinity of residential areas. It is not known exactly what the water requirements of ancient cotton plants were; they may have been less water-requiring than modern cotton crops, although irrigation remained essential under such hyper-arid climate ([Bouchaud and Tallet, 2020](#)).

The archaeological and isotope data leads us to conclude that most of the cotton was likely grown and processed on site during the period of occupation at Hegra—increasing in amount through time ([Bouchaud et al., 2018](#)). Although not exclusive to the al-ʿUlā region, the defined local strontium isotope ranges from modern plants and water do not contradict but rather support the archaeological evidence. Hegra, and the Nabateans who inhabited the site, appear to have played a critical role in the introduction/spread of cotton into the oasis of Arabia which would have required specific expertise i.e., growing, picking, ginning and spinning. It is not yet possible to say from existing information if the cotton was produced solely to meet local demand or if it was produced to surplus, making it a cash crop for widespread distribution. Given the capability of cotton production with irrigation systems and the key location of the site within trading networks, it is easily conceivable that the cotton produced on-site contributed to regional trade, potentially even entering wider Arabian and even Egyptian, Indian, and Mediterranean economies. Concurrently, cotton textiles could have been both produced on site, with some material being imported—possibly due to differing characteristics/value of imported fabrics.

The radiocarbon dates from Hegra pre-date and overlap in chronology with cotton finds at Mleiha on the Oman Peninsula ([Ryan et al., 2021](#)). Although they are broadly contemporaneous sites, there is a clear difference in the relationship with cotton at each of these settlements. With the exception of the textual mention of cotton growing in Bahrain during the 4th c. BCE (Theophrastus, *Historia plantarum*: 4.4.8) ([Amigues, 2010](#)), the cotton remains at Hegra represent the earliest production site of cotton on the Arabian Peninsula. The vast majority of radiocarbon and relative dates, combined with strontium isotope values, indicate that cotton production blossomed from the end of the 1st c. CE to the end of the occupation of the site, at the turn of the 5th c. CE and that it was also cultivated in the neighboring site of Dadan during the 5th–6th c. CE. While the full extent to which cotton growth and trade were taking place remains to be determined, this represents the earliest evidence for cotton production to date in western Arabia. In comparison, cuneiform texts show that cotton grew in several places in Mesopotamia during the 1st mill. BCE while the first secure evidence of cotton production we have in north-eastern Africa (Central Sudan and Western oasis of Egypt) dates back to the 1st–2nd c. CE ([Bagnall, 2008](#); [Clapham and Rowley-Conwy, 2009](#); [Fuller, 2014](#), see synthesis in [Bouchaud et al., 2018](#)). Our study demonstrates the first multi-proxy evidence for cotton production

in Arabia in Pre-Islamic times and offers a new milestone into the complex history of cotton diffusion through the Ancient world.

Data availability statement

The original contributions presented in the study are included in the article/[Supplementary Material](#), further inquiries can be directed to the corresponding author.

Author contributions

SR: Conceptualization, Data curation, Formal Analysis, Investigation, Methodology, Project administration, Validation, Visualization, Writing–original draft, Writing–review and editing. ED: Data curation, Formal Analysis, Methodology, Resources, Validation, Writing–review and editing. AD: Formal Analysis, Writing–review and editing. PD: Data curation, Formal Analysis, Resources, Writing–review and editing. VB: Investigation, Methodology, Resources, Writing–review and editing. AG: Formal Analysis, Writing–review and editing. ML: Data curation, Formal Analysis, Resources, Validation, Visualization, Writing–review and editing. JR: Investigation, Writing–review and editing. VD: Investigation, Resources, Writing–review and editing. PDP: Resources, Writing–review and editing. LN: Resources, Writing–review and editing. AZ: Conceptualization, Data curation, Funding acquisition, Investigation, Methodology, Project administration, Resources, Validation, Writing–original draft. CB: Conceptualization, Data curation, Funding acquisition, Investigation, Methodology, Project administration, Resources, Validation, Writing–original draft.

Funding

The authors declare financial support was received for the research, authorship, and/or publication of this article. The study was part of the ECO-SEED project directed by Charlène Bouchaud (CNRS) and the WAO (Past, present and future Water resources in Al-Ula Oasis) project, both funded by the French Agency for the Development of AIUla (AFALULA).

Acknowledgments

We wish to thank AFALULA and the Royal Commission for AIUla for their support. We thank the members of the excavation team from the Archaeological mission of Madā'in Sālih and Dadan for their contribution. We also thank Louise Bordier for assistance with Quadrupole-ICP-MS measurements (pre-dilutions for Neptune), as well as the ECHOMICADAS team from LSCE for graphitization and AMS measurement (notably, Nadine Tisnerat-Laborde and François Thil). Thanks to Michel Lemoine and Olivier Tombret from AASPE for their assistance with sample preparation. Imen Khabouchi and H el ene Mariot are thanked for their help in groundwater sampling and for their technical support in strontium analyses at CEREGE.

Conflict of interest

The authors declare that the research was conducted in the absence of any commercial or financial relationships that could be construed as a potential conflict of interest.

Publisher's note

All claims expressed in this article are solely those of the authors and do not necessarily represent those of their affiliated

organizations, or those of the publisher, the editors and the reviewers. Any product that may be evaluated in this article, or claim that may be made by its manufacturer, is not guaranteed or endorsed by the publisher.

Supplementary material

The Supplementary Material for this article can be found online at: <https://www.frontiersin.org/articles/10.3389/feart.2023.1257482/full#supplementary-material>

References

- Altherr, R., Mertz-Kraus, R., Volker, F., Kreuzer, H., Henjes-Kunst, F., and Lange, U. (2019). Geodynamic setting of Upper Miocene to Quaternary alkaline basalts from Harrat al 'Uwayrid (NW Saudi Arabia): constraints from K–Ar dating, chemical and Sr–Nd–Pb isotope compositions, and petrological modeling. *Lithos* 330–331, 120–138. doi:10.1016/j.lithos.2019.02.007
- Amigues, S. (2010). *Théophraste. Recherches sur les plantes: à l'origine de la botanique*. Paris, Belin: L'Histoire.
- Arnold, E. R., Hartman, G., Greenfield, H. J., Shai, I., Babcock, L. E., and Maier, A. M. (2016). Isotopic evidence for early trade in animals between Old Kingdom Egypt and Canaan. *PLoS One* 11, e0157650. doi:10.1371/journal.pone.0157650
- Bagnall, R. S. (2008). SB 6.9025, Cotton, and the economy of the small oasis. *Bull. Am. Soc. Papyrol.* 45.
- Benson, L. V., Hattori, E. M., Taylor, H. E., Poulson, S. R., and Jolie, E. A. (2006). Isotope sourcing of prehistoric willow and tule textiles recovered from western Great Basin rock shelters and caves - proof of concept. *J. Archaeol. Sci.* 33, 1588–1599. doi:10.1016/j.jas.2006.02.012
- Bentley, R. A. (2006). Strontium isotopes from the Earth to the archaeological skeleton: a review. *J. Archaeol. Method Theory* 13, 135–187. doi:10.1007/s10816-006-9009-x
- Bergfjord, C., Mannering, U., Frei, K. M., Gleba, M., Scharff, A. B., Skals, I., et al. (2012). Nettle as a distinct Bronze Age textile plant. *Sci. Rep.* 2, 664–4. doi:10.1038/srep00664
- Betts, A., van Der Borg, K., de Jong, A., McClintock, C., and Van Strydonck, M. (1994). Early cotton in north Arabia. *J. Archaeol. Sci.* 21, 489–499. doi:10.1006/jasc.1994.1049
- Bouchaud, C. (2015). Agrarian legacies and innovations in the nabataean territory. *Archaeosciences, Rev. d'Archéométrie* 39, 103–124. doi:10.4000/archeosciences.4421
- Bouchaud, C., Clapham, A., and Newton, C. (2018). "Cottoning on to cotton (gossypium sp.) in Arabia and Africa during antiquity," in *Plants and people in the african past plants* (Berlin, Germany: Springer).
- Bouchaud, C., Sachet, I., Dal Prà, P., Delhopyal, N., Douaud, R., and Leguilloux, M. (2015). New discoveries in a Nabataean tomb. Burial practices and 'plant jewellery' in ancient Hegra (Madā'in Sālih, Saudi Arabia). *Arab. Archaeol. Epigr.* 26, 28–42. doi:10.1111/aae.12047
- Bouchaud, C., and Tallet, G. (2020). "L'intégration du coton au sein des économies agraires antiques: un marqueur discret d'innovation," in *Le changement dans les économies antiques*. Editors F. Lerouxel and J. Zurbach (Bordeaux: Ausonius), 227–263.
- Bouchaud, C., Tengberg, M., and Prà, P. D. (2011). Cotton cultivation and textile production in the Arabian Peninsula during antiquity; the evidence from Madā'in Sālih (Saudi Arabia) and Qal'at al-Bahrain (Bahrain). *Veg. Hist. Archaeobot.* 2011. doi:10.1007/s00334-011-0296-0
- Bouchaud, C., Yvanez, E., and Wild, J. P. (2019). Tightening the thread from seed to cloth. New enquiries in the archaeology of Old World cotton. *Tendre un fil de la graine à l'habit. Nouvelles recherches sur l'archéologie du coton dans l'Ancien Monde: l'apport de l'interdisciplinarité*. *Rev. D'ethnoécologie*. 2019. doi:10.4000/ethnoecologie.4501
- Bronk Ramsey, C. (2020). *OxCal [WWW document]*. Available at: <https://c14.arch.ox.ac.uk/oxcal.html> (Accessed January 11, 2021).
- Brown, G. F., Jackson, R. O., Bogue, R. G., and Elberg, E. L. (1963). *Geology of the northwestern hijaz quadrangle, kingdom of Saudi Arabia*. Saudi Arabia: U.S. Geological Survey.
- Buzon, M. R., and Simonetti, A. (2013). Strontium isotope (87Sr/86Sr) variability in the Nile Valley: identifying residential mobility during ancient Egyptian and Nubian sociopolitical changes in the New Kingdom and Napatan periods. *Am. J. Phys. Anthropol.* 151, 1–9. doi:10.1002/ajpa.22235
- Capo, R. C., Stewart, B. W., and Chadwick, O. A. (1998). Strontium isotopes as tracers of ecosystem processes: theory and Methods. *Geoderma* 82, 197–225. doi:10.1016/s0016-7061(97)00102-x
- Charloux, G., Bouchaud, C., Durand, C., Gerber, Y., and Studer, J., 2018. Living in Madā'in Sālih/Hegra during the late pre-Islamic period. The excavations of Area 1 in the ancient city., in: J. Jansen van Rensburg and S. J. Power T, *Proceedings of the seminar for arabian studies*. Archaeopress, Oxford, pp. 47–65.
- Clapham, A., and Rowley-Conwy, P. (2009). "The archaeobotany of cotton (gossypium sp. L.) in Egypt and nubia with special reference to qasr ibrim, Egyptian nubia," in *From foragers to farmers. Papers in honour of gordon C. Hillman*. Editors A. Fairbairn and E. Weiss (Oxford: Oxbow Books), 244–253.
- Courbon, P. (2008). Les puits nabatéens de Mad in āli (arabie saoudite). *Arab. Archaeol. Epigr.* 19, 48–70. doi:10.1111/j.1600-0471.2007.00288.x
- Decker, M. (2009). Plants and progress: rethinking the islamic agricultural revolution. *J. World Hist.*, 208–226. doi:10.5040/9781474220118.ch-008
- Dominguez-Delmás, M., Rich, S., Traoré, M., Hajj, F., Poszwa, A., Akhmetzyanov, L., et al. (2020). Tree-ring chronologies, stable strontium isotopes and biochemical compounds: towards reference datasets to provenance Iberian shipwreck timbers. *J. Archaeol. Sci. Rep.* 34, 102640. doi:10.1016/j.jasrep.2020.102640
- English, N. B., Betancourt, J. L., Dean, J. S., and Quade, J. (2001). Strontium isotopes reveal distant sources of architectural timber in Chaco Canyon, New Mexico. *Proc. Natl. Acad. Sci. U. S. A.* 98, 11891–11896. doi:10.1073/pnas.211305498
- Evans, J. A., Montgomery, J., Wildman, G., and Boulton, N. (2010). Spatial variations in biosphere 87Sr/86Sr in Britain. *J. Geol. Soc. Lond.* 167, 1–4. doi:10.1144/0016-76492009-090
- Frei, K. M., Berghé, I. V., Frei, R., Mannering, U., and Lyngstrøm, H. (2010). Removal of natural organic dyes from wool-implications for ancient textile provenance studies. *J. Archaeol. Sci.* 37, 2136–2145. doi:10.1016/j.jas.2010.02.012
- Frei, K. M., and Bjerregaard, L. (2017). "Provenance investigations of raw materials in pre-Columbian textiles from Pachacamac; strontium isotope analyses," in *PreColumbian textile conference VII/jornadas de Textiles PreColombinos VII*. Editor L. B. Peters (Lincoln, NE: Zea Books), 387–397. doi:10.13014/K25D8Q1X
- Frei, K. M., Frei, R., Mannering, U., Gleba, M., Nosch, M. L., and Lyngstrøm, H. (2009a). Provenance of ancient textiles: a pilot study evaluating the strontium isotope system in wool. *Archaeometry* 51, 252–276. doi:10.1111/j.1475-4754.2008.00396.x
- Frei, K. M., Mannering, U., Kristiansen, K., Allentoft, M. E., Wilson, A. S., Skals, I., et al. (2015). Tracing the dynamic life story of a Bronze age female. *Sci. Rep.* 5, 10431. doi:10.1038/srep10431
- Frei, K. M., Mannering, U., Vanden Berghe, I., and Kristiansen, K. (2017). Bronze Age wool: provenance and dye investigations of Danish textiles. *Antiquity* 91, 640–654. doi:10.15184/aqy.2017.64
- Frei, K. M., Skals, I., Gleba, M., and Lyngstrøm, H. (2009b). The Huldremose Iron Age textiles, Denmark: an attempt to define their provenance applying the strontium isotope system. *J. Archaeol. Sci.* 36, 1965–1971. doi:10.1016/j.jas.2009.05.007
- Fuks, D., Amichay, O., and Weiss, E. (2020). Innovation or preservation? Abbasid aubergines, archaeobotany, and the islamic green revolution. *Archaeol. Anthropol. Sci.* 12, 50. doi:10.1007/s12520-019-00959-5
- Fuller, D. Q. (2014). "Agriculture innovation and state collapse in Meroitic Nubia," in *Archaeology of african plant use*. Editors C. J. Stevens, S. Nixon, M. A. Murray, and D. Q. Fuller (United States: Left Coast Press), 165–177.
- Hajj, F., Poszwa, A., Bouchez, J., and Guérol, F. (2017). Radiogenic and "stable" strontium isotopes in provenance studies: a review and first results on archaeological wood from shipwrecks. *J. Archaeol. Sci.* 86, 24–49. doi:10.1016/j.jas.2017.09.005

- Hu, L., Chartrand, M. M. G., St-Jean, G., Lopes, M., and Bataille, C. P. (2020). Assessing the reliability of mobility interpretation from a multi-isotope hair profile on a traveling individual. *Front. Ecol. Evol.* 8. doi:10.3389/fevo.2020.568943
- Kerfant, C., and Dabrowski, V. (2017). "Cotton fibres and seeds at Mleiha: a cotton production centre in southeast Arabian peninsula during Late Pre-Islamic period?," in *Le coton dans l'Ancien monde: domestication, culture* (Commerce: Usage).
- Kulkarni, V. N., Khadi, B. M., Maralappanavar, M. S., Deshapande, L. A., and Narayanan, S. S. (2009). The worldwide gene pools of *Gossypium arboreum* L. and *G. herbaceum* L., and their improvement. *Genet. Genomics Cott.* 2009. doi:10.1007/978-0-387-70810-2_4
- Liu, L., Levin, M. J., Klimscha, F., and Rosenberg, D. (2022). The earliest cotton fibers and Pan-regional contacts in the Near East. *Front. Plant Sci.* 13, 1045554. doi:10.3389/fpls.2022.1045554
- Mahamat Nour, A., Vallet-Coulomb, C., Bouchez, C., Ginot, P., Doumnang, J. C., Sylvestre, F., et al. (2020). Geochemistry of the lake Chad tributaries under strongly varying hydro-climatic conditions. *Aquat. Geochem.* 26, 3–29. doi:10.1007/s10498-019-09363-w
- Perry, M. A., Jennings, C., and Coleman, D. S. (2017). Strontium isotope evidence for long-distance immigration into the Byzantine port city of Aila, modern Aqaba, Jordan. *Archaeol. Anthropol. Sci.* 9, 943–964. doi:10.1007/s12520-016-0314-3
- Pinta, É., Pacheco-Forés, S. I., Wallace, E. P., and Knudson, K. J. (2021). Provenancing wood used in the Norse Greenlandic settlements: a biogeochemical study using hydrogen, oxygen, and strontium isotopes. *J. Archaeol. Sci.* 131, 105407. doi:10.1016/j.jas.2021.105407
- Price, T. D., Burton, J. H., and Bentley, R. A. (2002). The characterization of biologically available strontium isotope ratios for the study of prehistoric migration. *Archaeometry* 1, 117–135. doi:10.1111/1475-4754.00047
- Ramsay, J. H., and Parker, S. T. (2016). A diachronic look at the agricultural economy at the Red Sea Port of Aila: an archaeobotanical case for hinterland production in arid environments. *Bull. Am. Sch. Orient. Res.* 376, 101–120. doi:10.5615/bullamerschoorie.376.0101
- Reimer, P. J., Austin, W. E. N., Bard, E., Bayliss, A., Blackwell, P. G., Bronk Ramsey, C., et al. (2020). The IntCal20 northern hemisphere radiocarbon age calibration curve (0–55 cal kBP). *Radiocarbon* 62, 725–757. doi:10.1017/RDC.2020.41
- Reynolds, A. C., Betancourt, J. L., Quade, J., Patchett, P. J., Dean, J. S., and Stein, J. (2005). $^{87}\text{Sr}/^{86}\text{Sr}$ sourcing of ponderosa pine used in Anasazi great house construction at Chaco Canyon, New Mexico. *J. Archaeol. Sci.* 32, 1061–1075. doi:10.1016/j.jas.2005.01.016
- Ryan, S. E., Dabrowski, V., Dapoiny, A., Gauthier, C., Douville, E., Tengberg, M., et al. (2021). Strontium isotope evidence for a trade network between southeastern Arabia and India during Antiquity. *Sci. Rep.* 11, 303–310. doi:10.1038/s41598-020-79675-3
- Sanfilippo, A., Sani, C., Rasul, N. M. A., Stewart, I. C. F., Vigliotti, L., Widinly, N., et al. (2021). Hidden but ubiquitous: the pre-rift continental mantle in the red sea region. *Front. Earth Sci.* 9. doi:10.3389/feart.2021.699460
- Snoeck, C., Schulting, R. J., Brock, F., Rodler, A. S., Van Ham-Meert, A., Mattioli, N., et al. (2021). Testing various pre-treatments on artificially waterlogged and pitch-contaminated wood for strontium isotope analyses. *Front. Ecol. Evol.* 8, 1–10. doi:10.3389/fevo.2020.589154
- Squatriti, P. (2014). Of seeds, seasons, and seas: andrew Watson's medieval agrarian revolution forty years later. *J. Econ. Hist.* 74, 1205–1220. doi:10.1017/S0022050714000904
- Stanish, C., Tantaleán, H., and Knudson, K. (2018). Feasting and the evolution of cooperative social organizations circa 2300 B.P. in Paracas culture, southern Peru. *Proc. Natl. Acad. Sci. U. S. A.* 115, E6716–E6721. doi:10.1073/pnas.1806632115
- Stantis, C., Kharobi, A., Maaranen, N., Nowell, G. M., Bietak, M., Prell, S., et al. (2020). Who were the Hyksos? Challenging traditional narratives using strontium isotope ($^{87}\text{Sr}/^{86}\text{Sr}$) analysis of human remains from ancient Egypt. *PLoS One* 15, e0235414. doi:10.1371/journal.pone.0235414
- Tengberg, M. (2012). Beginnings and early history of date palm garden cultivation in the Middle East. *J. Arid. Environ.* 86, 139–147. doi:10.1016/j.jaridenv.2011.11.022
- Van Ham-Meert, A., Rodler, A. S., Waight, T. E., and Daly, A. (2020). Determining the Sr isotopic composition of waterlogged wood – cleaning more is not always better. *J. Archaeol. Sci.* 124, 105261. doi:10.1016/j.jas.2020.105261
- Viot, C. (2019). Domestication et diversification variétale des cotons cultivés (*Gossypium* sp.) de l'Ancien Monde dans l'Antiquité. *Rev. D'ethnologie.* 2019. doi:10.4000/ethnologie.4404
- Watson, A. M. (1974). The arab agricultural revolution and its diffusion, 700–1100. *J. Econ. Hist.* 34, 8–35. doi:10.1017/S0022050700079602
- Watson, A. M. (1981). "A medieval green revolution: new crops and farming techniques in the Early Islamic world," in *The Islamic Middle East 700–1900: studies in economic and social history*. Editor A. L. Udovitch (Princeton: The Darwin Press).
- Watson, A. M. (1983). *Agricultural innovation in the early Islamic world: the diffusion of crops and farming techniques*. Cambridge: Cambridge University Press.
- Wild, J. P. (1997). Cotton in roman Egypt: some problems of origin. *Al-Rafidan* 18, 287–298.
- Willmes, M., Mcmorrow, L., Kinsley, L., Armstrong, R. A., Aubert, M., Eggins, S., et al. (2014). The IRHUM (Isotopic Reconstruction of Human Migration) database - bioavailable strontium isotope ratios for geochemical fingerprinting in France. *Earth Syst. Sci. Data* 6, 117–122. doi:10.5194/essd-6-117-2014
- Wozniak, M. M., and Belka, Z. (2022). The provenance of ancient cotton and wool textiles from nubia: insights from technical textile analysis and strontium isotopes. *J. Afr. Archaeol.* 150, 202–216. doi:10.1163/21915784-bja10019
- Yeghicheyan, D., Grinberg, P., Alleman, L. Y., Belhadj, M., Causse, L., Chmeleff, J., et al. (2021). Collaborative determination of trace element mass fractions and isotope ratios in AQUA-1 drinking water certified reference material. *Anal. Bioanal. Chem.* 413, 4959–4978. doi:10.1007/s00216-021-03456-8

Supplementary Information for

Strontium isotopes reveal Pre-Islamic cotton cultivation in Arabia

Saskia E. Ryan^{1,2*}, Eric Douville², Arnaud Dapoigny², Pierre Deschamps³, Vincent Battesti⁴, Abel Guihou³, Matthieu Lebon⁵, Jérôme Rohmer⁶, Vladimir Dabrowski¹, Patricia Dal Prà⁷, Laïla Nehmé⁸, Antoine Zazzo^{1#}, Charlène Bouchaud^{1#}

¹Archéozoologie, Archéobotanique: Sociétés, Pratiques et Environnements (AASPE, UMR 7209), Muséum national d'Histoire naturelle, CNRS, CP56, 55 rue Buffon, 75005, Paris, France.

²Laboratoire des Sciences du Climat et de l'Environnement, LSCE/IPSL, UMR CEA-CNRS-UVSQ, Université Paris-Saclay, F-91191 Gif-sur-Yvette, France.

³Aix Marseille Univ, CNRS, IRD, INRAE, CEREGE, Aix-en-Provence, France.

⁴Éco-anthropologie (EA UMR 7206), CNRS, Muséum national d'Histoire naturelle, Université Paris Cité, Musée de l'Homme 17 place du Trocadéro 75016 Paris, France.

⁵Histoire naturelle de l'Homme Préhistorique (HNHP, UMR 7194), Muséum national d'Histoire naturelle, CNRS, UPVD, Musée de l'Homme, 17 place du Trocadéro, 75016, Paris, France.

⁶CNRS, UMR 8167 Orient & Méditerranée, Ivry-sur-Seine, France.

⁷Institut national du patrimoine, 124 rue Henri Barbusse, 93300 Aubervilliers, France.

⁸Orient & Méditerranée (UMR 8167), CNRS, 27, rue Paul Bert - 94204 Ivry sur Seine.

#Equal contribution.

*Corresponding author: Saskia E. Ryan

Email: ryans22@tcd.ie

This file includes:

Appendices 1-3

Figures S1–S12

Tables S1–S5

SI References

Appendix 1

1 Site and samples

1.1 Archaeological context

The site of Hegra includes oasis gardens which were irrigated through a dense network of wells and a residential area built on an alluvial plain. The latter was surrounded by monumental rock-cut tombs carved into the cliffs of sandstone outcrops during the Nabataean period. The evidence from the excavations shows that the residential area of ancient Hegra was occupied as early as the 5th century BCE. The Nabataeans did not settle there before the mid-first c. BCE, i.e. long after they had made Petra, Jordan, their capital city. This movement southward is probably due to their desire to keep control over the trade of myrrh, frankincense and other aromatics at a time when maritime trade routes through the Red Sea became widely used (Nehmé, 2021). The study of the charred plant macro-remains highlights the presence of an oasis agrosystem dominated by date palm (*Phoenix dactylifera* L.) cultivation and composed of other fruit trees such as pomegranate (*Punica granatum* L.), olive (*Olea europaea* L.) and vines (*Vitis vinifera* L.), as well as cereals and pulses (see details in Bouchaud (2015)). The archaeobotanical assemblage includes hundreds of carbonized cotton seeds unearthed during the excavations in the residential area, with a time distribution spanning several centuries from the late 1st to the early 4th c. CE. Desiccated textiles were uncovered inside the funerary chambers of the monumental Nabataean tombs, originally part of shrouds. Many are made of linen and wool, but several cotton textiles were also identified (Bouchaud et al., 2015, 2011).

Dadan (mod. al-Khurraybah) is located c. 15 km to the south of Hegra, in the al-'Ulā oasis, at the bottom of a deep valley flanked by steep sandstone mountains. The archaeological site lies on the eastern side of the valley, at the foot of high sandstone cliffs, slightly above the modern oasis gardens of the alluvial plain. Its main component is a c. 9 ha wide tell, settled from the 3rd mill. BCE to the early 1st mill. BCE. It represents the ancient city of Dadan, which reached its peak during the 1st mill. BCE when it became the capital of two successive North-Arabian kingdoms (Dadan and Liḥyān) and a major hub on the 'Incense Road' (Macdonald, 1997). About 900 m to the south of this tell, a recent survey by the Dadan Archaeological Project has revealed a Late Antique settlement made of several scattered stone mounds. A test excavation carried out in the Autumn 2021 on the largest of these mounds (Excavation Area E) uncovered part of a large building, including a central courtyard with hydraulic installations. The function of this building remains unknown, but at least two architectural phases have been identified, the first of which was radiocarbon-dated to the 3rd/early 4th centuries CE. The second architectural phase was sealed by a very thick layer of dump containing a large amount of ceramic, faunal and botanical remains (Rohmer et al., 2022), including cotton seeds. According to radiocarbon analyses performed on the cotton seeds, this dump dates from the 5th/6th c. CE, i.e. the very poorly known period just before the advent of Islam.

1.2 Geological context

The sites of Hegra and Dadan are located in north-western Arabia, straddling the Arabian platform and the Arabian shield (for detailed geological history see Brown et al. (1989)). The region comprises a wide variety of geological bedrocks ranging from Precambrian to Quaternary in age but broadly, three main groupings can be made: volcanic-sedimentary sequences associated with the Precambrian Arabian Shield, relatively homogeneous Lower Palaeozoic (Cambro-Ordovician) sandstone and Cenozoic volcanic fields (*harrat*) (Coleman et al., 1983). Notably, the Harrat al-Rahah-'Uwayrid, an expansive volcanic plateau is exposed directly north-west and west of Hegra (Camp and Roobol, 1992; Coleman, 1993). The Nabataean rock-cut tombs are carved in Cambrian Quweira sandstone outcrops.

1.3 Material under study

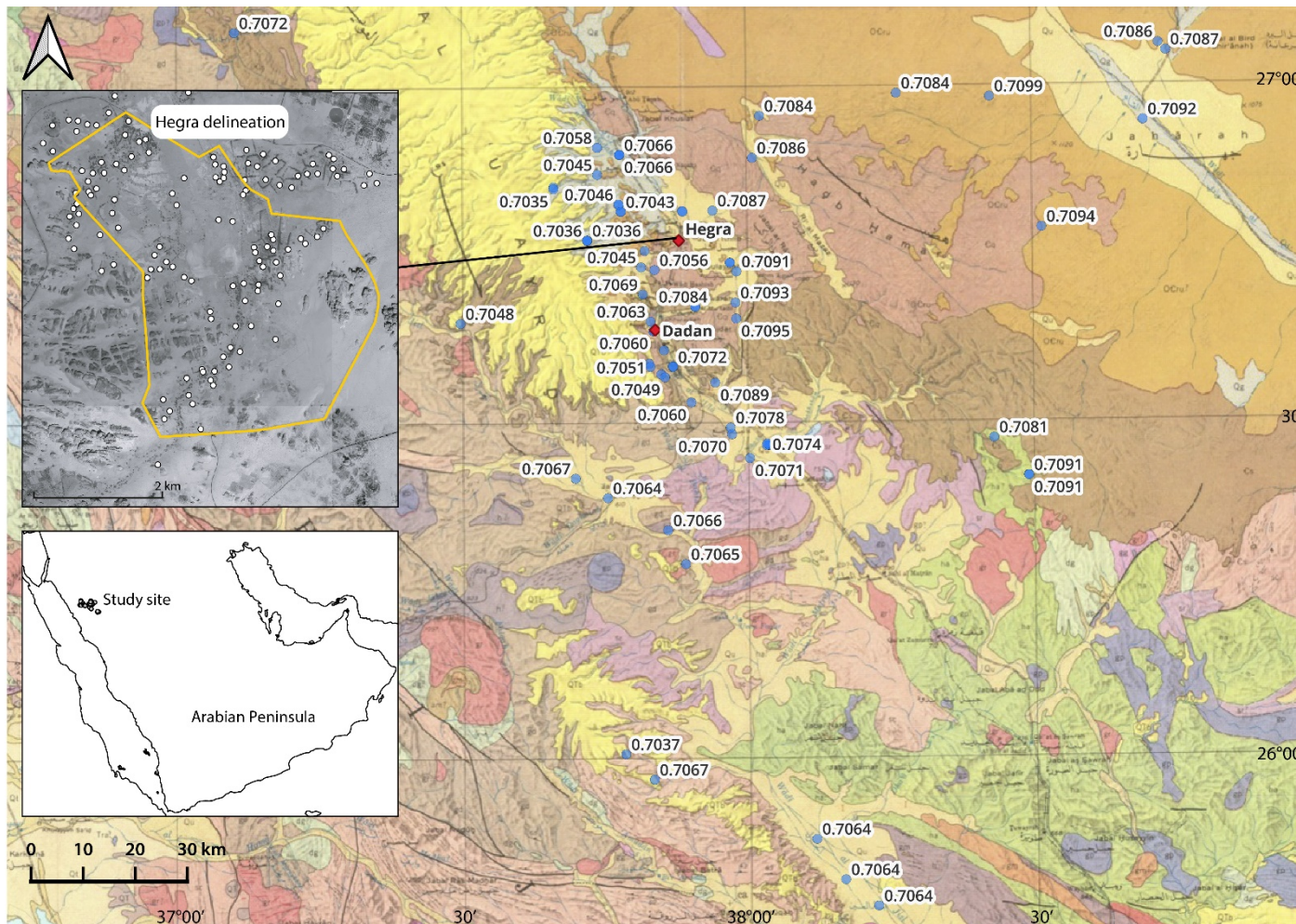
From Hegra, nineteen archaeological charred cotton seeds and twelve uncharred pieces of textile (with two duplicates), including 8 composed of cotton (example in **Figure S1**), one of a linen/cotton blend and three of wool, were selected for Sr isotope analysis. The textiles are all plain weave and Z-twist. Furthermore, an archaeological caryopsis of barley ($n = 1$) and date palm seeds ($n = 2$) were analysed, as well as two samples of wood charcoal from the Amaranthaceae family. Since they are abundant in the archaeobotanical record at sites in Arabia, they are taken to have been grown locally. Four archaeological cotton textiles from the site of Mleiha and their corresponding acid leachates were previously analysed for their strontium isotope composition (Ryan et al., 2021) and here, were analysed for strontium concentrations.

From the Late Antique area E of Dadan, nine archaeological charred cotton seeds were analysed as well as tamarisk ($n = 7$) and date palm ($n = 2$) charcoal remains.



Figure S1. Desiccated cotton textile, plain weave, Z-twist. The yellow circle indicates the sampling area for analysis.

In order to gauge the local isotope range that exists within the region, fifteen modern vegetation samples were gathered from the wadi al-'Ulā and the sandy plain that encompasses both the sites of Hegra and Dadan. More distally (see **Fig. 1** for map of sites), twenty-two modern plants were collected across the region to inform on the wider, regional geochemical variability covering different geological landscapes (**SI Appendix, Table S1**). Seventy-one well and spring water samples were collected across the wadi al-'Ulā and its surrounds to define the regional water strontium isotope signature of the Saq aquifer that feeds the area (**SI Appendix, Table S2**). See **Figure S2** for distribution of the archaeological wells at Hegra.



Geologic Explanation

Qu	Gravel, sand, silt and clay, undifferentiated	Quaternary
QTb	Basalt and andesite	Tertiary
OCru	Ram and Umm Sahn sandstones, undivided	Cambrian and Ordovician
Cq	Quweira sandstone	Cambrian
Cs	Siq sandstone	Cambrian
gm	Granite	Precambrian
sr	Shammar rhyolite	
gp	Granite or syenite	
h	Hadiyah slate	
ha	Halaban andesite	
gr	Granite	
gg	Granite and granite gneiss	
dg	Dioite and granodiorite	Precambrian
gd	Greenstone	
●	Groundwater sample	
◆	Archaeological site	

Figure S2. Geological map of the study area with strontium isotope values of sampled groundwater (USGS basemap (Brown et al., 1963) <https://pubs.er.usgs.gov/publication/i204A>). Not all groundwater datapoints are visible on the map as, for the sake of clarity, overlaying labels are not shown. For the comprehensive dataset, please see Supplementary Information, Table S2. Upper inset map shows the geographical location and distribution of archaeological wells (white circle) at the site of Hegra. The yellow line represents the “administrative” limit the archaeological site © Madâ'in Sâlih Archaeological project. Cartography based on Th. Arnoux & L. Nehmé, 2006

Strontium isotope values of archaeological and modern plant material

Lab ID	Field ID	Type	Site	Material	Identification	Scientific name	$^{87}\text{Sr}/^{86}\text{Sr}^*$	2 sigma uncertainty	Northing	Easting	Chronology (14C: 2 sigmas)	Archaeological context
SR8911	gm2	Modern		Wood	Remth	<i>Haloxylon salicornicum</i> (M oq.) Bunge ex Boiss.	0.70809	0.00002	26.8661	37.2461	Modern	
SR8910	gm1	Modern		Wood	Taily Weed	<i>Ochradenus baccatus</i> Delile	0.70809	0.00002	26.8392	37.2617	Modern	
SR8912	gm3	Modern		Wood	Raetam	<i>Retama raetam</i> (Forssk.) Webb & Berthel	0.70807	0.00002	26.8125	37.2436	Modern	
SR8909	gr3	Modern		Wood	Sumac	<i>Searsia tripartita</i> (Ucria) Moffett	0.70969	0.00002	26.5842	37.1997	Modern	
SR8908	gr2	Modern		Wood	Raetam	<i>Retama raetam</i> (Forssk.) Webb & Berthel	0.70769	0.00002	26.5725	37.1969	Modern	
SR8907	gr1	Modern		Wood	Remth	<i>Haloxylon salicornicum</i> (M oq.) Bunge ex Boiss.	0.71044	0.00002	26.5831	37.1736	Modern	
SR8897	mh3	Modern		Wood	Arabian boxthorn	<i>Lycium shawii</i> Roem. & Schult.	0.70752	0.00002	26.5572	37.2661	Modern	
SR8899	Qu1	Modern		Wood	White saxaul	<i>Haloxylon persicum</i> Bunge ex Boiss. & Buhse	0.70683	0.00002	26.6867	37.4081	Modern	
SR8890	gd1	Modern		Wood	Remth	<i>Haloxylon salicornicum</i> (M oq.) Bunge ex Boiss.	0.70789	0.00002	26.6031	37.4539	Modern	
SR8892	gd3	Modern		Wood	Red Acacia	<i>Vachellia seyal</i> (Delile) P.J.H.Hurter	0.70711	0.00002	26.5619	37.5231	Modern	
SR8891	gd2	Modern		Wood	Umbrella thorn acacia	<i>Vachellia tortilis</i> (Forssk.) Galasso & Banfi	0.70727	0.00002	26.5328	37.5522	Modern	
SR8900	Qu2	Modern		Wood	Remth	<i>Haloxylon salicornicum</i> (M oq.) Bunge ex Boiss.	0.70709	0.00002	26.4247	37.8756	Modern	
SR8913	ha1	Modern		Wood	Twisted acacia	<i>Vachellia tortilis</i> subsp. <i>raddiana</i> (Savi) Kyal. & Boatwr.	0.70773	0.00002	26.1436	38.5342	Modern	
SR8915	ha3	Modern		Wood	Umbrella thorn acacia	<i>Vachellia tortilis</i> (Forssk.) Galasso & Banfi	0.70650	0.00002	26.1197	38.4442	Modern	
SR8914	ha2	Modern		Wood	Twisted acacia	<i>Vachellia tortilis</i> subsp. <i>raddiana</i> (Savi) Kyal. & Boatwr	0.70774	0.00002	26.1725	38.4417	Modern	
SR8894	sr2	Modern		Wood	Remth	<i>Haloxylon salicornicum</i> (M oq.) Bunge ex Boiss.	0.70765	0.00002	26.3344	37.9892	Modern	
SR8893	sr1	Modern		Wood	Remth	<i>Haloxylon salicornicum</i> (M oq.) Bunge ex Boiss.	0.70756	0.00002	26.3336	37.9981	Modern	
SR8895	QTb1	Modern		Wood	Ferula	<i>Ferula sinaica</i> Boiss.	0.70779	0.00002	26.6717	37.8333	Modern	

SR8896	QTb3	Modern		Wood	Lusak	<i>Forsskaolea tenacissima</i> L.	0.70775	0.00002	26.6344	37.8756	Modern	
SR8905	Cs3	Modern		Wood	Remth	<i>Haloxylon salicornicum</i> (M oq.) Bunge ex Boiss.	0.70815	0.00002	26.7167	38.1686	Modern	
SR8906	Cq1	Modern		Wood	Remth	<i>Haloxylon salicornicum</i> (M oq.) Bunge ex Boiss.	0.70817	0.00002	26.7544	38.2558	Modern	
SR8901	Cs1	Modern		Wood	Umbrella thorn acacia	<i>Vachellia tortilis</i> (Forssk.) Hayne	0.70854	0.00002	26.6233	38.0744	Modern	
SR8904	Cs2	Modern		Wood	Remth	<i>Haloxylon salicornicum</i> (M oq.) Bunge ex Boiss.	0.70888	0.00002	26.6558	38.0675	Modern	
9825	DD2	Modern		Wood	Common bean	<i>Phaseolus vulgaris</i> L.	0.70865	0.00011	26.852	37.962	Modern	
9826	DD3	Modern		Wood	Gourd	<i>Cucurbita</i> sp.	0.70687	0.00011	26.615	37.930	Modern	
9827	DD4	Modern		Wood	Gumbo	<i>Abelmoschus esculentus</i> (L.) Moench	0.70849	0.00011	26.664	37.939	Modern	
9828	DD5	Modern		Wood	Real Mustard Tree	<i>Salvadora persica</i> L.	0.70722	0.00005	27.125	37.168	Modern	
9829	DD6	Modern		Wood	Date palm	<i>Phoenix dactylifera</i> L.	0.70511	0.00005	26.698	37.910	Modern	
9830	DD7	Modern		Wood	Date palm	<i>Phoenix dactylifera</i> L.	0.70836	0.00005	26.661	37.926	Modern	
9831	DD8	Modern		Wood	Date palm	<i>Phoenix dactylifera</i> L.	0.70672	0.00007	26.614	37.928	Modern	
9832	DD9	Modern		Wood	Khip	<i>Leptadenia pyrotechnica</i> (Forssk.) Decne.	0.70775	0.00007	26.664	37.927	Modern	
9833	DD9	Modern		Wood		<i>Leptadenia pyrotechnica</i> (Forssk.) Decne.	0.70773	0.00007				
9834	Duplicate DD9 Triplicate	Modern		Wood		<i>Leptadenia pyrotechnica</i> (Forssk.) Decne.	0.70778	0.00001				
SR 389 ^T	MS_FLOR A14	Modern		Wood	Cotton	<i>Gossypium barbadense</i> L.	0.70843	0.00002	26.825	37.9547	Modern	
SR 390	MS_RETAMA	Modern		Wood	Raetam	<i>Retama raetam</i> (Forssk.) Webb & Berthel	0.70729	0.00002	26.8063	37.9449	Modern	
SR 391	MS_ACAC IA1 Teflon	Modern		Wood	Twisted acacia	<i>Vachellia tortilis</i> subsp. <i>raddiana</i> (Savi) Kyal. & Boatwr	0.70730	0.00002	26.8063	37.9449	Modern	
SR 392 ^T	MS_GOSS YP	Modern		Wood	Cotton	<i>Gossypium barbadense</i> L.	0.70839	0.00002	26.825	37.9547	Modern	
SR 393	MS_TAMAR	Modern		Wood	Athel tamarisk	<i>Tamarix aphylla</i> (L.), Karst.	0.70753	0.00002	26.7789	37.9442	Modern	
SR 394	MS_ACAC IA2	Modern		Wood	Twisted acacia	<i>Vachellia tortilis</i> subsp. <i>raddiana</i> (Savi) Kyal. & Boatwr	0.70735	0.00002	26.8251	37.9546	Modern	
SR 397	MS_25103_AMAR	Archaeological	Hegra	Charcoal	Amaranth family	Amaranthaceae	0.70680	0.00002			mid 4th-6th c. CE	Fireplace
SR 398	MS_90024_PHOEN	Archaeological	Hegra	Seed	Date palm	<i>Phoenix dactylifera</i> L.	0.70680	0.00002			1st c. CE	Floor, ashy deposit

SR 417	MS 80166 Phoenix dactylifera	Archaeologi cal	Hegra	Seed	Date palm	<i>Phoenix dactylifera</i> L.	0.70712	0.00002			3rd-4th c. CE	Dump
SR 418	MS 10216 Amarantha ceae	Archaeologi cal	Hegra	Charco al	Amaranth family	Amaranthaceae	0.70714	0.00002			Early 2nd- mid 1st c. BCE	Ashy layer
SR 460	MS 10151 Hordeum V.	Archaeologi cal	Hegra	Seed	Barley	<i>Hordeum vulgare</i> L.	0.70740	0.00002			4th-5th c. CE	Floor
9864	DDN C 375 Bot1 1	Archaeologi cal	Dadan	Charco al	Athel tamarisk	<i>Tamarix aphylla</i> (L.), Karst.	0.70917	0.00002	26.6457	37.9145		
9865	DDN C 375 Bot1 2	Archaeologi cal	Dadan	Charco al	Athel tamarisk	<i>Tamarix aphylla</i> (L.), Karst.	0.70913	0.00004	26.6457	37.9145		
9866	DDN C 375 Bot1 3	Archaeologi cal	Dadan	Charco al	Athel tamarisk	<i>Tamarix aphylla</i> (L.), Karst.	0.70997	0.00004	26.6457	37.9145		
9867	DDN C 375 Bot1 4	Archaeologi cal	Dadan	Charco al	Athel tamarisk	<i>Tamarix aphylla</i> (L.), Karst.	0.70860	0.00002	26.6457	37.9145		
9868	DDN C 375 Bot1 5	Archaeologi cal	Dadan	Charco al	Athel tamarisk	<i>Tamarix aphylla</i> (L.), Karst.	0.70981	0.00002	26.6457	37.9145		
9869	DDN C 375 Bot1 6	Archaeologi cal	Dadan	Charco al	Athel tamarisk	<i>Tamarix aphylla</i> (L.), Karst.	0.70963	0.00004	26.6457	37.9145		
9870	DDN C 375 Bot1 7	Archaeologi cal	Dadan	Charco al	Athel tamarisk	<i>Tamarix aphylla</i> (L.), Karst.	0.70959	0.00002	26.6457	37.9145		
9862	DDN E 39 Bot 1 Phoenix	Archaeologi cal	Dadan	Charco al	Date palm	<i>Phoenix dactylifera</i> L.	0.70608	0.00002	26.6457	37.9145		
9863	DDN E 39 Bot 1 Phoenix	Archaeologi cal	Dadan	Charco al	Date palm	<i>Phoenix dactylifera</i> L.	0.70612	0.00003	26.6457	37.9145		
SR402	MS 80166	Archaeologi cal	Hegra	Seed	Cotton	<i>Gossypium</i> sp.	0.70716	0.00002			249-409 cal CE	Dump
SR403	MS 80022	Archaeologi cal	Hegra	Seed	Cotton	<i>Gossypium</i> sp.	0.71518	0.00005			2nd-4th c. CE	Dump
SR404	MS 10061	Archaeologi cal	Hegra	Seed	Cotton	<i>Gossypium</i> sp.	0.70795	0.00002			83-237 cal. CE (indirect)	Fireplace
SR405	MS 10153	Archaeologi cal	Hegra	Seed	Cotton	<i>Gossypium</i> sp.	0.70726	0.00002			4th-5th c. CE	Fireplace
SR406	MS 10061	Archaeologi cal	Hegra	Seed	Cotton	<i>Gossypium</i> sp.	0.70696	0.00002			83-237 cal. CE (indirect)	Fireplace
SR407	MS 60641	Archaeologi cal	Hegra	Seed	Cotton	<i>Gossypium</i> sp.	0.70703	0.00002			4th-6th c. CE	Ashy layer
SR408	MS 10156	Archaeologi cal	Hegra	Seed	Cotton	<i>Gossypium</i> sp.	0.70810	0.00002			4th-5th c. CE	Fireplace
SR409	MS 80106	Archaeologi cal	Hegra	Seed	Cotton	<i>Gossypium</i> sp.	0.70720	0.00002			120-306 cal CE	Ashy layer

SR410	MS 60641	Archaeological	Hegra	Seed	Cotton	<i>Gossypium</i> sp.	0.71411	0.00005			4th-6th c. CE	Ashy layer
SR411	MS 60639	Archaeological	Hegra	Seed	Cotton	<i>Gossypium</i> sp.	0.70703	0.00002			4th-6th c. CE	Ashy layer
SR 416	MS 10151	Archaeological	Hegra	Seed	Cotton	<i>Gossypium</i> sp.	0.70783	0.00002			4th-5th c. CE	Floor
SR 451	MS 20026	Archaeological	Hegra	Seed	Cotton	<i>Gossypium</i> sp.	0.70797	0.00002			120-306 cal CE (indirect)	Oven filling
SR 452	MS 25017	Archaeological	Hegra	Seed	Cotton	<i>Gossypium</i> sp.	0.71298	0.00005			end 2nd-early 4th c. CE	Destruction
SR 453	MS 25203	Archaeological	Hegra	Seed	Cotton	<i>Gossypium</i> sp.	0.70726	0.00002			end 2nd-5th c. CE	Unknown
SR 454	MS 60612	Archaeological	Hegra	Seed	Cotton	<i>Gossypium</i> sp.	0.70828	0.00002			4th-6th c. CE	Basin filling
SR 455	MS 60612	Archaeological	Hegra	Seed	Cotton	<i>Gossypium</i> sp.	0.70727	0.00002			4th-6th c. CE	Basin filling
SR 456	MS 80129	Archaeological	Hegra	Seed	Cotton	<i>Gossypium</i> sp.	0.70715	0.00002			2nd-4th c. CE	Oven filling
SR 457	MS 60628	Archaeological	Hegra	Seed	Cotton	<i>Gossypium</i> sp.	0.71466	0.00004			4th-6th c. CE	Basin filling
SR 459	MS 90021	Archaeological	Hegra	Seed	Cotton	cf. <i>Gossypium</i> sp.	0.70695	0.00002				Occupation floor
9848	DDN E 39 Bot 1	Archaeological	Dadan	Seed	Cotton	<i>Gossypium</i> sp.	0.70611	0.00002	26.6457	37.9145	415-547 cal CE	
9850	DDN E 39 Bot 1	Archaeological	Dadan	Seed	Cotton	<i>Gossypium</i> sp.	0.70701	0.00004	26.6457	37.9145	415-547 cal CE	
9851	DDN E 39 Bot 1	Archaeological	Dadan	Seed	Cotton	<i>Gossypium</i> sp.	0.70617	0.00003	26.6457	37.9145	415-547 cal CE	
9852	DDN E 39 Bot 1	Archaeological	Dadan	Seed	Cotton	<i>Gossypium</i> sp.	0.70677	0.00004	26.6457	37.9145	415-547 cal CE	
9853	DDN E 39 Bot 1	Archaeological	Dadan	Seed	Cotton	<i>Gossypium</i> sp.	0.70735	0.00002	26.6457	37.9145	415-547 cal CE	
9854	DDN E 39 Bot 1	Archaeological	Dadan	Seed	Cotton	<i>Gossypium</i> sp.	0.70639	0.00002	26.6457	37.9145	415-547 cal CE	
9855	DDN E 39 Bot 1	Archaeological	Dadan	Seed	Cotton	<i>Gossypium</i> sp.	0.70669	0.00004	26.6457	37.9145	415-547 cal CE	
9856	DDN E 39 Bot 1	Archaeological	Dadan	Seed	Cotton	<i>Gossypium</i> sp.	0.70681	0.00004	26.6457	37.9145	415-547 cal CE	
9857	DDN E 39 Bot 1	Archaeological	Dadan	Seed	Cotton	<i>Gossypium</i> sp.	0.70790	0.00006	26.6457	37.9145	415-547 cal CE	
SR 414	MS 50432_T41	Archaeological	Hegra	Textile	Cotton	<i>Gossypium</i>	0.70855	0.00002			126 - 236 cal CE	Tomb IGN 97
SR 415	MS 50432_T41 (duplicate)	Archaeological	Hegra	Textile	Cotton	<i>Gossypium</i>	0.70880	0.00002			126 - 236 cal CE	Tomb IGN 97

SR 428	MS 50045_T05	Archaeologi cal	Hegra	Textile	Cotton	<i>Gossypium</i>	0.70828	0.00002	1st-3rd c. CE	Tomb IGN 20
SR 429	MS 50045_T06	Archaeologi cal	Hegra	Textile	Cotton	<i>Gossypium</i>	0.70823	0.00002	1st-3rd c. CE	Tomb IGN 20
SR 430	MS 50045_T09	Archaeologi cal	Hegra	Textile	Cotton	<i>Gossypium</i>	0.70832	0.00002	1st-3rd c. CE	Tomb IGN 20
SR 431	MS50432_ T43	Archaeologi cal	Hegra	Textile	Cotton	<i>Gossypium</i>	0.70869	0.00002	1st-3rd c. CE	Tomb IGN 97 maybe of the same unit as 50432_T41.
SR 432	MS50432_ T32	Archaeologi cal	Hegra	Textile	Cotton	<i>Gossypium</i>	0.70831	0.00002	47 cal BCE-76 cal. CE	Tomb IGN 97
SR 433	MS 50432_T27	Archaeologi cal	Hegra	Textile	Cotton	<i>Gossypium</i>	0.70853	0.00002	1st-3rd c. CE	Tomb IGN 97
SR 440	MS 50045_T06 (duplicate)	Archaeologi cal	Hegra	Textile	Cotton	<i>Gossypium</i>	0.70826	0.00002	1st-3rd c. CE	Tomb IGN 20
SR 441	MS 50240_T11	Archaeologi cal	Hegra	Textile	Hair (wool?)		0.70916	0.00002	1st-3rd c. CE	Tomb IGN 117
SR 442	MS 50240_L2	Archaeologi cal	Hegra	Textile	Hair (wool?)		0.70871	0.00003	1st-3rd c. CE	Tomb IGN 117
SR 443	MS 50432_T62	Archaeologi cal	Hegra	Textile	Wool		0.71287	0.00002	1st-3rd c. CE	Tomb IGN 97
SR 444	MS 50432_T51	Archaeologi cal	Hegra	Textile	Linen (and cotton?)		0.70910	0.00002	1st-3rd c. CE	Tomb IGN 97
SR 445	MS 50052_T17	Archaeologi cal	Hegra	Textile	Cotton	<i>Gossypium</i>	0.70830	0.00001	1st-3rd c. CE	Tomb IGN 117

Table S1. Strontium isotope values and chronology of study material. *Corrected ratio, ^TDerived from the same plot. The radiocarbon ages are calibrated using the Oxcal 4.4. software and the IntCal20 atmospheric curve (Bronk Ramsey, 2020; Reimer et al., 2020).

Strontium isotope values of ground and well water

CEREGE Study	Sample name	Samp. N°	ULA Samp. Code	Type	Longitude	Latitude	87Sr/86Sr	Err 87Sr/86Sr
Mars 2019	Abo Maher forage Mission Mars 2019	#1	19-01	Forage	37.854983	26.827837	0.70435	0.00002
Mars 2019	Shalal source Mission Mars 2019	#2	19-02	Source	37.79714	26.783332	0.70362	0.00002
Mars 2019	Hegra forage Mission Mars 2019	#3	19-03	Forage	37.960597	26.829077	0.70828	0.00002
Mars 2019	New Hegra Mission Mars 2019	#4	19-04	Forage	38.043238	26.749567	0.70829	0.00002
Mars 2019	Assany Mission Mars 2019	#5	19-05	Forage	38.081235	26.911088	0.70857	0.00002
Mars 2019	Al-Qatar source Mission Mars 2019	#6	19-06	Source	38.559787	26.423204	0.70907	0.00002
Mars 2019	Awarosh forage Mission Mars 2019	#7	19-07	Forage	37.57834	26.655001	0.70481	0.00002
Mars 2019	Mughreyra airport Mission Mars 2019	#8	19-08	Forage	38.111078	26.468546	0.70743	0.00002
Mars 2019	Mansorah Al-'Ulā Mission Mars 2019	#9	19-09	Forage	37.945293	26.588706	0.70724	0.00002
Mars 2019	Dadan forage Mission Mars 2019	#10	19-10	Forage	37.912882	26.644204	0.70641	0.00002

Mars 2019	Elephant rock forage Mission Mars 2019	#11	19-11	Forage	37.983587	26.681674	0.70836	0.00002
Janvier 2020	WELL 1 Mission Janvier 2020	#13	20-02	Forage	37.906463	26.658494	0.70626	0.00002
Janvier 2020	Qa'a Al-Haj Mission Janvier 2020	#15	20-04	Forage	38.054317	26.663339	0.70948	0.00002
Janvier 2020	Hani Bishr Mission Janvier 2020	#16	20-05	Forage	38.054616	26.736072	0.70913	0.00002
Janvier 2020	Grager-02 Mission Janvier 2020	#17	20-06	Forage	37.890046	26.742166	0.70445	0.00002
Janvier 2020	Balawi Mission Janvier 2020	#22	20-11	Forage	37.851416	26.838055	0.70450	0.00002
Janvier 2020	Balawi new Mission Janvier 2020	#23	20-12	Forage	37.850741	26.839075	0.70457	0.00002
Janvier 2020	Hmed2 Mission Janvier 2020	#25	20-14	Forage	37.852153	26.91544	0.70661	0.00002
Janvier 2020	Almehobi Mission Janvier 2020	#26	20-15	Forage	37.813961	26.926197	0.70580	0.00002
Janvier 2020	Shalal Mission Janvier 2020	#27	20-16	Source	37.79714	26.783332	0.70361	0.00002
Sept 2021	21-01 Dadan 01	#28	21-01	Forage	37.912882	26.644204	0.70637	0.00002
Sept 2021	21-02 Dadan 02	#29	21-02	Forage	37.910881	26.644142	0.70601	0.00002
Sept 2021	21-03 Dadan 01	#30	21-03	Forage	37.912882	26.644204	0.70641	0.00002
Sept 2021	21-04 Al Hajra 01	#31	21-04	Forage	37.96128	26.828136	0.70825	0.00002
Sept 2021	21-05 Al Hajra 02	#32	21-05	Forage	38.012992	26.82983	0.70869	0.00002
Sept 2021	21-06 Mantaza 02	#33	21-06	Forage	37.9131	26.7381	0.70561	0.00002

Sept 2021	21-07 Al Jadida 01	#34	21-07	Forage	38.781363	27.090721	0.70865	0.00002
Sept 2021	21-08 Al Jadida 02 B43	#35	21-08	Forage	38.7945	27.0792	0.70867	0.00002
Sept 2021	21-09 Al Jadida 03	#36	21-09	Forage	38.7556	26.9719	0.70919	0.00002
Sept 2021	21-10 Ramm 01	#37	21-10	Forage	38.01815	26.56445	0.70890	0.00002
Sept 2021	21-11 Mogayra 01	#38	21-11	Forage	38.111078	26.468546	0.70744	0.00002
Sept 2021	21-12 Mogayra 02	#39	21-12	Forage	38.10698	26.468311	0.70749	0.00002
Sept 2021	21-13 Mogayra 03	#40	21-13	Forage	38.10818	26.470631	0.70738	0.00002
Sept 2021	21-14 Elephant	#41	21-14	Forage	37.98357	26.6816	0.70834	0.00002
Sept 2021	21-15 Motadel	#42	21-15	Forage	38.05286	26.6881	0.70927	0.00002
Sept 2021	21-16 NewHegra	#43	21-16	Forage	38.043238	26.749567	0.70846	0.00002
Sept 2021	21-17 Sader 02	#44	21-17	Forage	37.904147	26.593532	0.70509	0.00002
Sept 2021	21-18 Sader 03	#45	21-18	Forage	37.906227	26.588794	0.70511	0.00002
Sept 2021	21-19 Sader 07	#46	21-19	Forage	37.925017	26.577036	0.70475	0.00002
Sept 2021	21-20 Sader 09	#47	21-20	Forage	37.931535	26.572559	0.70487	0.00002
Sept 2021	21-21 B50	#48	21-21	Forage	38.580853	26.806576	0.70937	0.00002
Sept 2021	21-22 Mewa B56	#49	21-22	Forage	38.4905	27.0069	0.70987	0.00002

Sept 2021	21-23 B53	#50	21-23	Forage	38.3296	27.0113	0.70838	0.00002
Sept 2021	21-24 Abo Maher 01	#51	21-24	Forage	37.854983	26.827837	0.70432	0.00002
Sept 2021	21-25 Mogayra 05	#52	21-25	Forage	38.078176	26.447959	0.70710	0.00002
Sept 2021	21-26 Al Jabena 02	#53	21-26	Forage	38.044798	26.495101	0.70777	0.00002
Sept 2021	21-27 Al Jabena 03	#54	21-27	Forage	38.047237	26.484894	0.70704	0.00002
Sept 2021	21-28 Ain Tharba 01	#55	21-28	Source	37.738732	26.865475	0.70364	0.00002
Sept 2021	21-29 Ain Tharba 02	#56	21-29	Source	37.738425	26.862494	0.70354	0.00002
Sept 2021	21-30 Aina Tharba 04	#57	21-30	Forage	37.814246	26.884643	0.70448	0.00002
Sept 2021	21-31-Elbley B37	#58	21-31	Forage	38.09365	26.97579	0.70836	0.00002
Sept 2021	21-32 Hmed 01 C#24	#59	21-32	Forage	37.852358	26.915642	0.70680	0.00002
Sept 2021	21-33 Hmed 02 C#25	#60	21-33	Forage	37.852126	26.915434	0.70665	0.00002
Sept 2021	21-34 Shalal TOP	#61	21-34	Source	37.796597	26.78322	0.70362	0.00002
Sept 2021	21-35 Malsan	#62	21-35	Forage	37.896006	26.767545	0.70458	0.00002
Sept 2021	21-36 Al Shara B21	#63	21-36	Forage	37.89301	26.70041	0.70688	0.00002
Sept 2021	21-37 Katar	#64	21-37	Source	38.559787	26.423204	0.70907	0.00002
Sept 2021	21-38 Farm Al Jamel	#65	21-38	Forage	38.499652	26.481244	0.70805	0.00002

Sept 2021	21-39 Al Azizya	#66	21-39	Forage	37.976971	26.533998	0.70598	0.00002
Sept 2021	21-40 Mansorah 02	#67	21-40	Forage	37.945191	26.589515	0.70695	0.00002
Sept 2021	21-41 Fadhla 02	#68	21-41	Forage	37.83295	26.385806	0.70636	0.00002
Sept 2021	21-42 Daf khal	#69	21-42	Forage	37.777262	26.416011	0.70674	0.00002
Sept 2021	21-43 Khocheba	#70	21-43	Forage	37.936943	26.336187	0.70656	0.00002
Sept 2021	21-44	#71	21-44	Forage	37.967672	26.28394	0.70647	0.00002
Sept 2021	21-45 Al Jadedah 01	#72	21-45	Forage	38.194357	25.858212	0.70641	0.00002
Sept 2021	21-46 Al Jadedah 02	#73	21-46	Forage	38.244132	25.795206	0.70643	0.00002
Sept 2021	21-47 Al Ayn	#74	21-47	Forage	38.301124	25.75459	0.70637	0.00002
Sept 2021	21-48 Aburaka	#75	21-48	Forage	37.187262	27.102788	0.70724	0.00002
Sept 2021	21-49 Al Bair 01	#76	21-49	Source	37.86461	25.989211	0.70372	0.00002
Sept 2021	21-50 Al Bair 02	#77	21-50	Source	37.914097	25.949789	0.70665	0.00002
Sept 2021	21-51 Slimane Citycenter	#78	21-51	Forage	37.929572	26.61423	0.70430	0.00002

Table S2. $^{87}\text{Sr}/^{86}\text{Sr}$ of ground and well water from the region of al-'Ulā, sampled between 04/2019-10/2021.

Appendix 2

2 FTIR Report

For all the samples, it proved difficult to isolate the residues present on the surface of the fibres. However, under a microscope, it was possible to focus the analyses on the different materials and to distinguish them from cellulose fibers. The analyses were carried out by Fourier transform infrared micro-spectrometry, in transmission mode (after pressing the sample in a diamond cell), on the infrared spectroscopy platform of the MNHN (UMR 7194).

Sample IGN20-50045-T6-F3

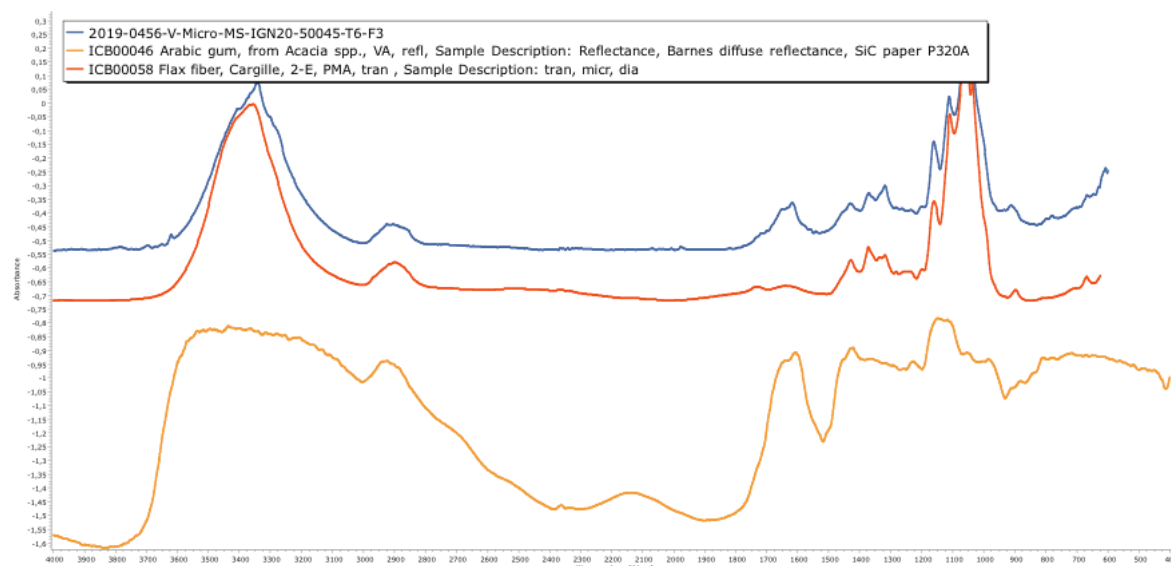


Figure S3. Infrared spectra obtained for sample IGN20-50045-T6-F3. It is almost exclusively composed of cellulose (Flax fiber – IRUG Spectral Database – ICB 00058), with some probable traces of a gum as shown by absorption bands between 1500-1800 cm^{-1} , potentially acacia gum (Flax fiber – IRUG Spectral Database – ICB 00046)

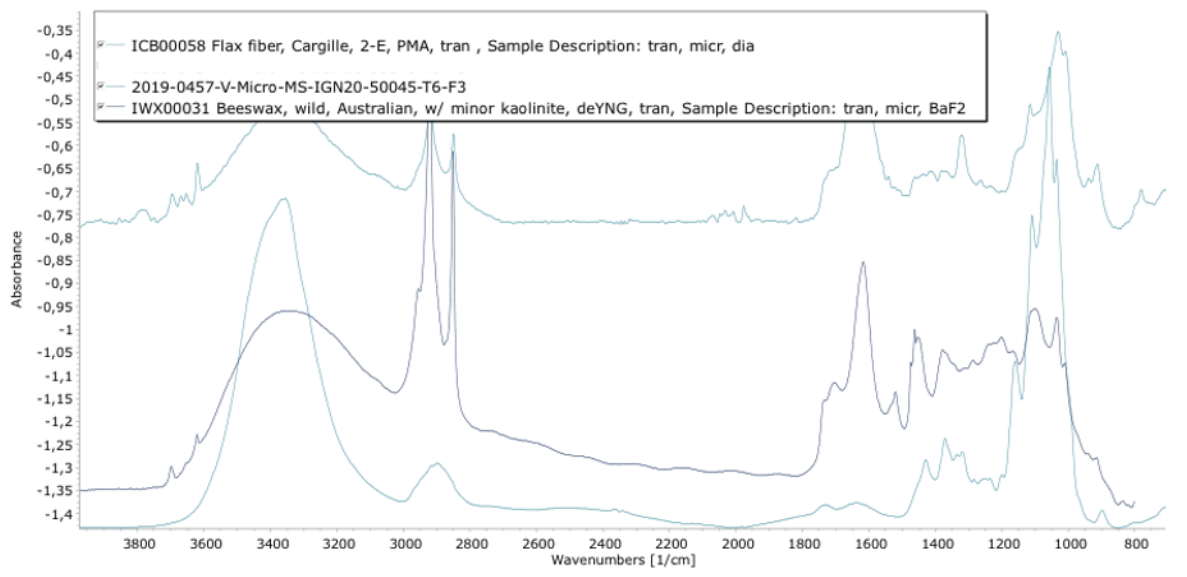


Figure S4. FTIR spectra obtained for sample IG20-50045-T6-F3. The spectra display the absorption bands of cellulose as well as clay (kaolinite). The presence of a wax is suggested by bands between 1800-1500 cm⁻¹ and high C-H absorption band between 2800 and 3100 cm⁻¹.

Sample IG97-50432-T32

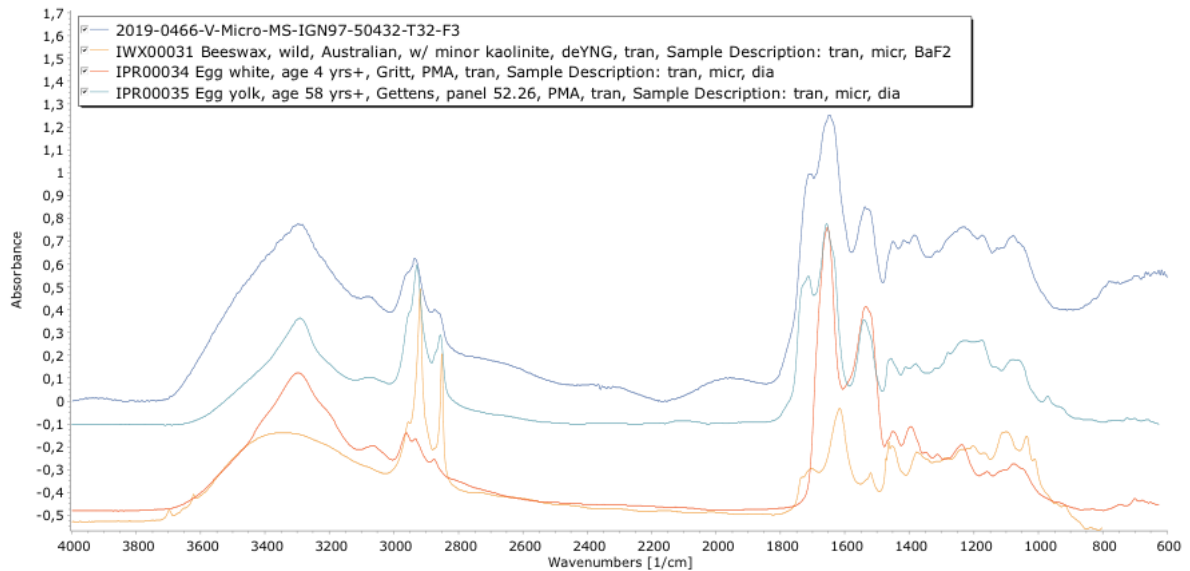


Figure S5. Sample IG97-50432-T32 is cellulose with a proteinaceous material. The band at 1720 cm⁻¹ corresponds with being a lipid, while the main band of proteins corresponds with the reference band for egg yolk.

Sample IGN20-50045-T5

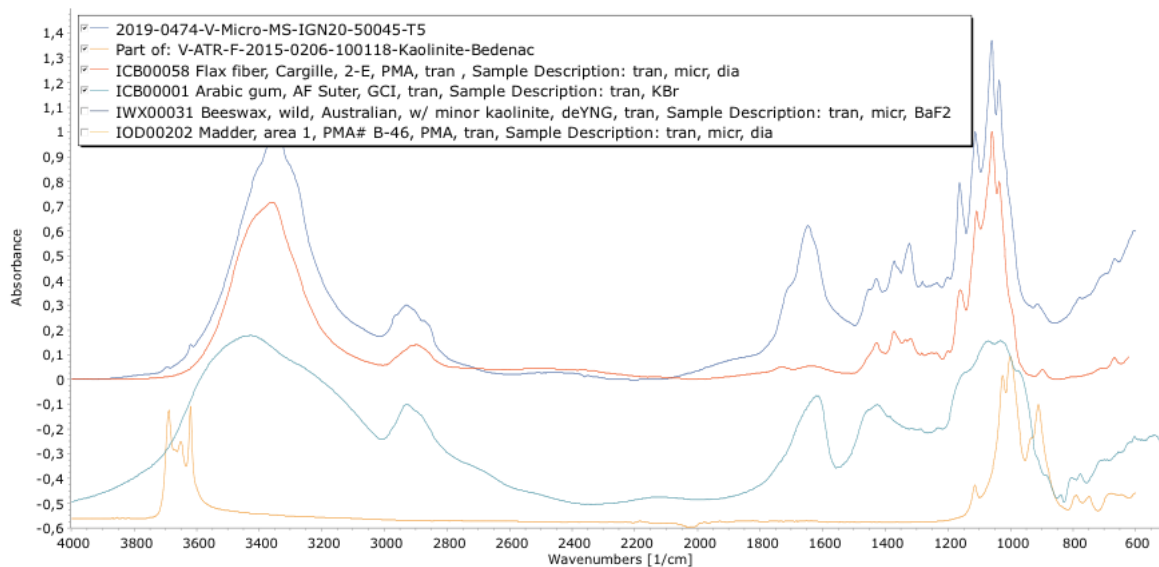


Figure S6. The spectra obtained on sample IGN20-50045-T5 suggest the presence of Kaolinite associated with the cellulose. Another organic material, probably a gum (eg. Arabic Gum) seems to be present.

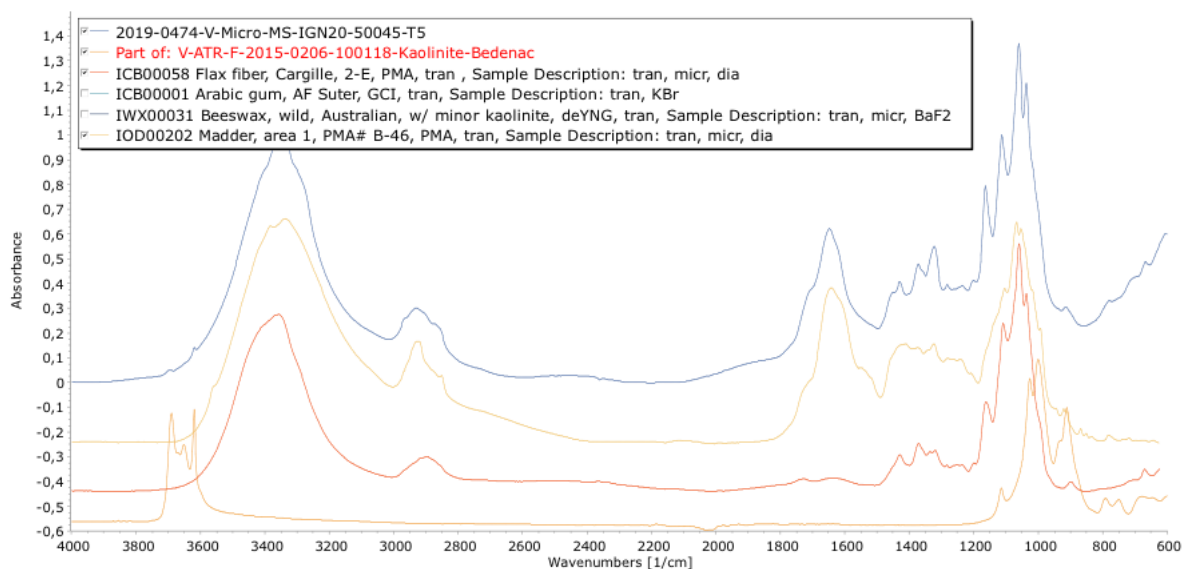


Figure S7. For sample IGN20-50045-T5, the potential presence of madder is evoked based on the good reference fit between 1500 and 1800 cm.

Sample IGN20-50032-T43

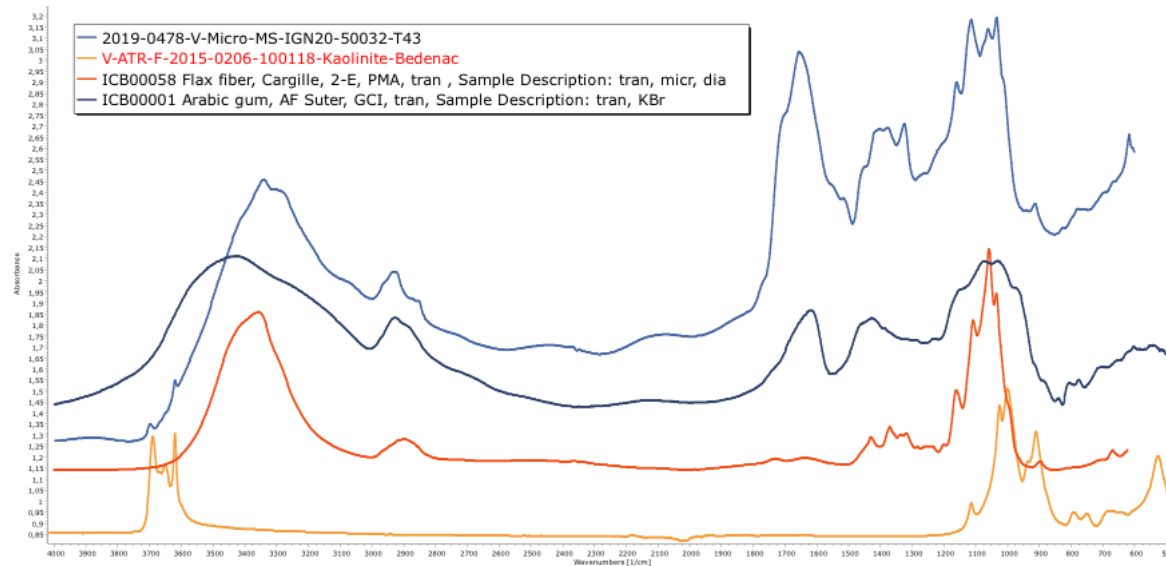


Figure S8. Infrared spectra obtained on sample IGN20-50032-T43 suggest the presence of kaolinite and Arabic gum, in association with the cellulose.

Sample IGN97-50432-T41

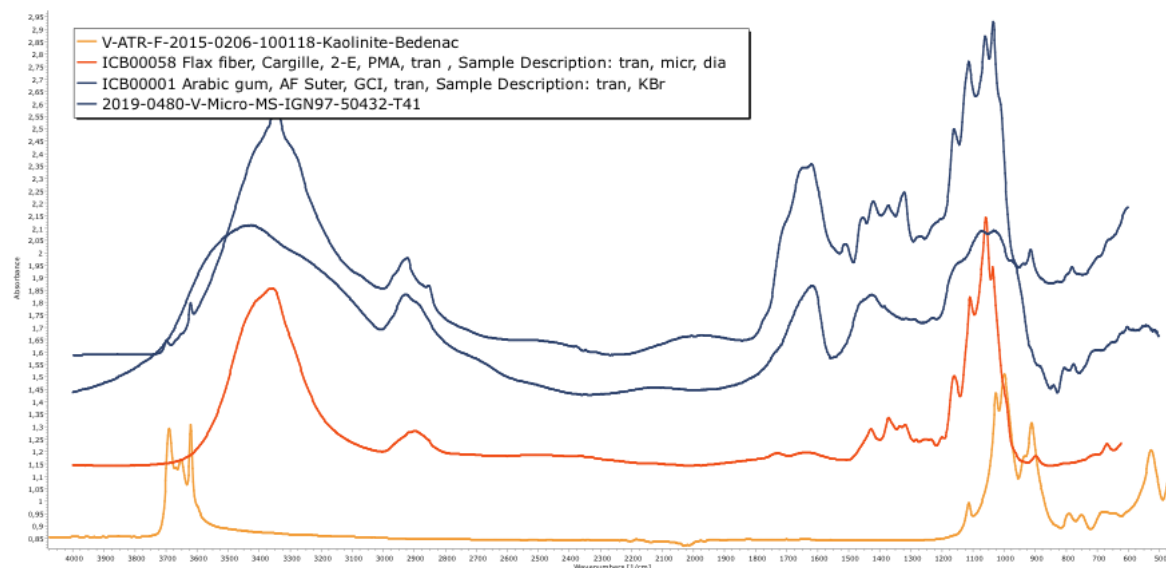


Figure S9. Infrared spectra obtained for sample IGN97-50432-T41 suggest the presence of kaolinite and Arabic gum, in association with the cellulose. The composition is close to that of sample IGN20-50032-T43 (above).

Sample IGN117-50240-T11

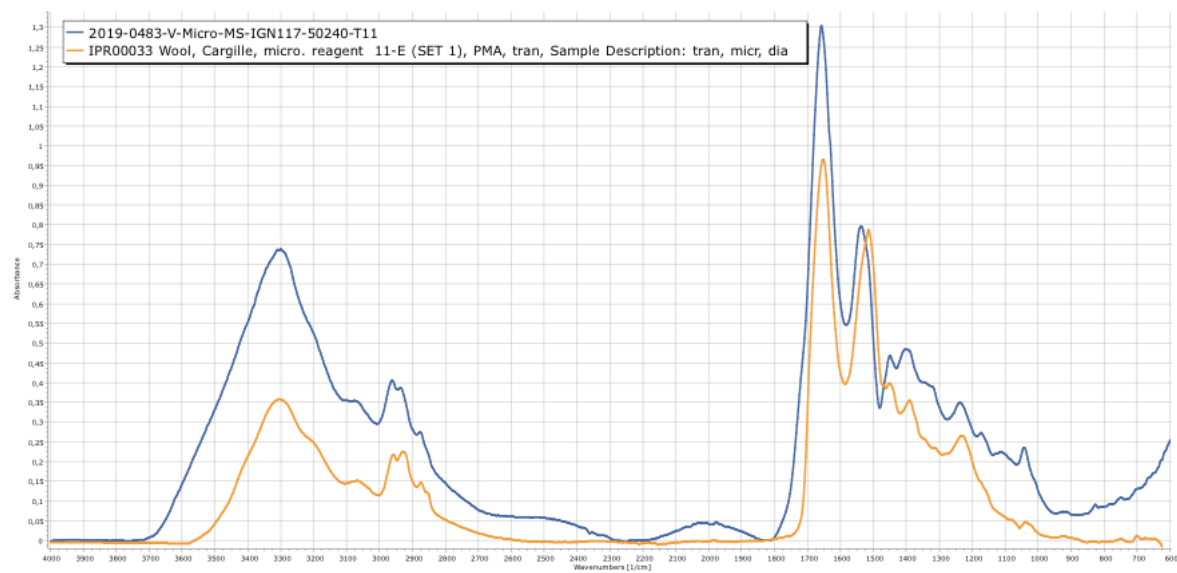


Figure S10. Spectra obtained for sample IGN117-50240-T11 confirm the proteinaceous nature of the material, seen here compared to the Wool IRUG spectral database.

Appendix 3

3 Pre-treatment of botanical remains: removal of contaminants by leaching

Exogenous Sr was removed from carbonized cotton seeds by leaching them in 5 ml 6 M HCl for 24 h, an adapted procedure of that found to be the most effective of several different leaches at removing some but not all contaminants (Styring et al., 2019). The solutions were centrifuged, the supernatant removed and the leached seeds were rinsed in ultrapure Milli-Q water three times and dried. In the case of the recovered textiles, FTIR analysis (**SI Appendix 2**) revealed the presence of gum (see **SI Appendix, Table S3**) on some of the textiles so a solvent leach was required to remove any potential lipid-based resin (Cequier-Sánchez et al., 2008). Dichloromethane-methanol (2:1, v/v) solution was added to each textile sample and allowed to sit at room temperature for an hour and then rinsed three times with ultrapure Milli-Q water. Microscopic inspection revealed the presence of sand grains embedded between the fibres. A room temperature 20% hydrofluoric (HF) acid leach for 1 h, under ultrasonic treatment, was used to remove these grains. Subsequently, the HF supernatant was removed, leaving behind the residual textile sample. This portion was then rinsed three times with ultrapure Milli-Q water. The same leaching procedure was used again with 1 M HCl in place of the HF. The residual textile was then dried, as were the leachates. This procedure followed an adapted method outlined in Frei and Bjerregaard (2017) (Ryan et al., 2021), which was designed to decontaminate textile samples of silicates that are rich in Sr.

Locus	Tomb	Year	Material	Fabric	Other comments	Twist	Dye	FTIR analysis
50432_T41	IGN 97	2014	Cotton	Tabby	Edge and fringes	Z	No	Mainly cellulose but probably associated with a gum (e.g. Arabic gum) and traces of clay
50045_T06	IGN 20		Cotton					
50045_T05	IGN 20	2008	Cotton	Tabby	Fringe	Z	See FTIR results	Mainly cellulose but probably associated with a gum (e.g. Arabic gum) and kaolinite. The presence of madder is also possible.
50045_T09	IGN 20	2008	Cotton	Tabby	Edge and fringes	Z	No	
50432_T43	IGN 97	2014	Cotton	Tabby		Z	No	Mainly cellulose but probably associated with gum (e.g. Arabic gum) and kaolinite.
50432_T32	IGN 97	2014	Cotton	Tabby				Cellulose with a proteinaceous

50432_T27	IGN 97	2014	Cotton	Rope			No	material that corresponds with the reference band for egg yolk.
50045_T06	IGN 20	2008	Cotton	Tabby		Z	No	Almost exclusively cellulose, with some probable traces of a gum (e.g. acacia gum)
50240_T11	IGN 117	2008	Hair (wool?)	Tabby			No	Proteineous in nature with spectral pattern similar to that of wool
50240_L02(1)	IGN 117	2008	Hair (wool?)	Tabby	Unidentified black substance (<i>Canarium?</i>)	S	Yes	
50432_T62	IGN 97	2014	Wool	Tabby	Unidentified black substance		No	
50432_T51	IGN 97	2014	Linen (and cotton?)				No	
50052_T17	IGN 20	2008	Cotton	Tabby	Strip		No	

Table S3. FTIR results from textile material.

Sample ID	Site	HCl leach			HF leach			Residual Textile		
		$^{87}\text{Sr}/^{86}\text{Sr}^{\text{T}}$	2σ uncertainty	Sr conc ppm	$^{87}\text{Sr}/^{86}\text{Sr}^{\text{T}}$	2σ uncertainty	Sr conc ppm	$^{87}\text{Sr}/^{86}\text{Sr}^{\text{T}}$	2σ uncertainty	Sr conc ppm
Sr 428	<u>Hegra</u>	0.70794	0.00002	1357	Run failed			0.70828	0.00002	99
Sr 429	<u>Hegra</u>	0.70752	0.00002	768	0.70849	0.00002	133	0.70823	0.00002	99
Sr 430	<u>Hegra</u>	0.70749	0.00002	764	0.70828	0.00002	131	0.70832	0.00002	48
Sr 431	<u>Hegra</u>	0.70720	0.00002	906	0.70795	0.00002	96	0.70869	0.00002	36
Sr 432	<u>Hegra</u>	0.70750	0.00002	1562	0.70786	0.00002	72	0.70831	0.00002	18
Sr 434*	Mleiha	0.70864	0.00002	32309	0.70889	0.00002	197	0.70884	0.00002	12
Sr 435*	Mleiha	0.70864	0.00002	28629	0.70916	0.00002	376	0.71122	0.00002	20
Sr 436*	Mleiha	0.70862	0.00002	9825	0.70871	0.00002	242	0.71039	0.00002	2
Sr 437*	Mleiha	0.70865	0.00002	12181	0.71327	0.00002	58	0.71413	0.00002	1

Table S4. $^{87}\text{Sr}/^{86}\text{Sr}$ and Sr concentrations of textile leachates and residues from Hegra and the site of Mleiha. ^TCorrected ratio + standard bracketing. *Isotope data from Ryan et al., 2021.

The HCl and HF acid leachate fractions and the residue textiles were found to have notably different strontium isotope ratios and concentrations, with less radiogenic strontium being removed with each leaching step relative to what remained in the residue (**SI Appendix, Table S4**). We include parallel published data from the site of Mleiha (Ryan et al., 2021) for comparison which highlights that not only are there differences noted between the cleaning steps but there is also a clear difference in residue values for selected samples here between the sites of Mleiha and Hegra (**SI Appendix, Figure S11**).

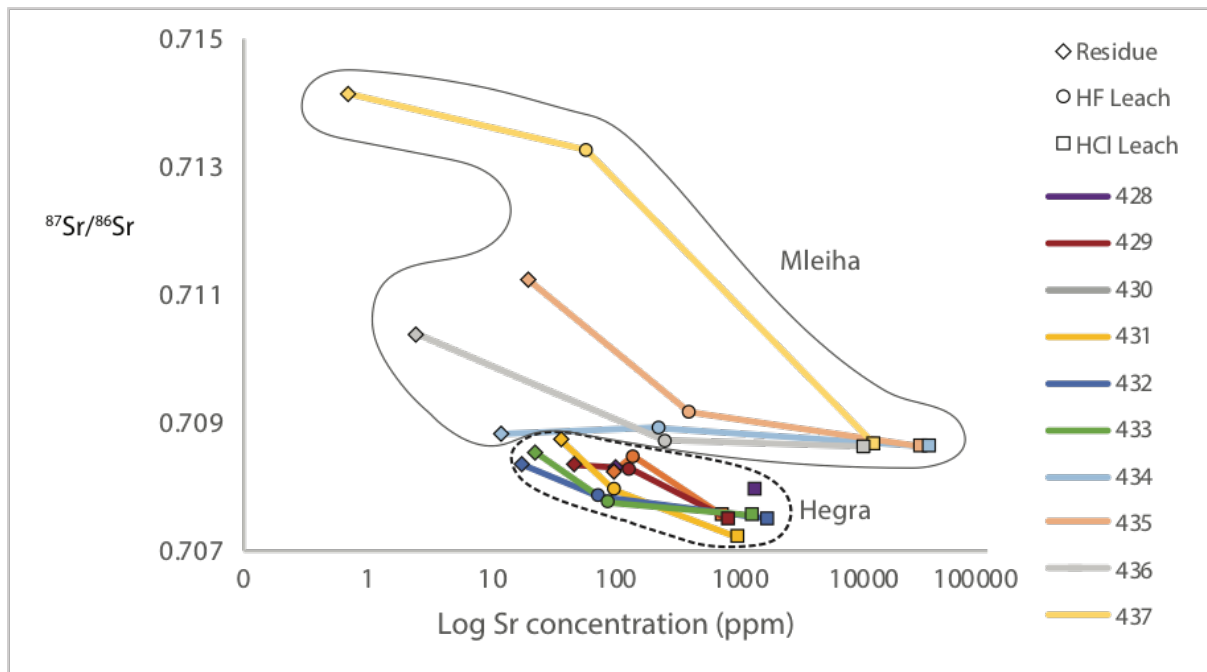


Figure S11. Strontium isotopes of the cotton textile leachates and residues, 4% uncertainty.

3.1 Observations on the removal of contaminants

When analysing the isotope composition of archaeological plant samples, diagenetic contamination is a concern. Microscopic analysis of the textiles showed that sand grains were embedded between the cotton fibres of the textiles. To remove the sand, acid leaching was required. To test the effectiveness of the decontamination of the ancient plant material, we examined the Sr concentrations and $^{87}\text{Sr}/^{86}\text{Sr}$ values of leachate fractions, as well as the residues.

After the solvent rinse to remove resins, there were two acid leaching methods employed here, which broadly followed those of previous studies: One for the textile materials (Frei et al., 2009) and one for the cotton seeds (Bogaard et al., 2014; Heier et al., 2009; Larsson et al., 2020; Styring et al., 2019). As the latter method has already been proven effective at removal of non-biogenic strontium, it is appropriate for use on the cotton seeds investigated here. The leaching method for the textiles has been studied in less depth and has for the most part been applied to wool, although there is at least one instance of its application to cotton textiles (Frei and Bjerregaard, 2017).

The archaeological residue textiles from Mleiha have more radiogenic and more variable strontium isotope values (Ryan et al., 2021) than those analysed as part of the current study from Hegra, despite both sites having comparable local strontium isotope baseline ranges. This shows that the difference in values of the textile residues is not an artefact of the method but that real differences are present as a function of the studied sites and their respective cotton provenance or production area.

It is crucial to be aware of the potential effects that incomplete removal of contaminants could have on the provenance interpretation. Incomplete removal of sand would result in an over-estimation of locally-grown cotton, as burial contamination would act to skew the strontium isotope signature towards that of the local region in which they were found. Examining the $^{87}\text{Sr}/^{86}\text{Sr}$ ratios and Sr concentrations of the leachate(s) aids with determining the effectiveness of contaminant removal. It is possible that the leachates were aggressive enough to remove not only the exogenous Sr but also the original internal (biogenic) Sr from the cotton and therefore the Sr concentration of the residues would not represent the entire Sr pool that was originally present in the living plant. Nonetheless, the chemical de-contamination method recovers the unfractionated $^{87}\text{Sr}/^{86}\text{Sr}$ ratios of the endogenous Sr that remains. Therefore, measurement of the Sr isotope composition of archaeological seeds and textiles can nonetheless provide an effective means of identifying cotton unlikely to have been cultivated in the local area. Confirming local origin is more difficult as contaminants and residues will have similar $^{87}\text{Sr}/^{86}\text{Sr}$ ratios and therefore, incomplete removal of contaminants would result in an overestimation of 'local' material/an underestimation of non-local material. As such, we recommend that caution should be exercised with the $^{87}\text{Sr}/^{86}\text{Sr}$ analyses of archaeological botanical samples from unknown regions of origin due to the possibility that the biogenic $^{87}\text{Sr}/^{86}\text{Sr}$ ratios could be altered by contamination from the (burial) environment. Ideally, the efficacy of the method should be independently evaluated using strontium concentrations. Here, the amount of strontium removed with each acid leaching step (HCl leachates have an average of 8947 ± 12090 SD ppm, HF leachates 141 ± 106 SD ppm) is magnitudes of order greater than the amount of residual strontium (average 36 ± 36 SD ppm) in the cotton textile. We deem the $^{87}\text{Sr}/^{86}\text{Sr}$ ratio of the cotton residues to be a useful provenance tool because: (1) the endogenous and exogenous Sr mostly have similar $^{87}\text{Sr}/^{86}\text{Sr}$ ratios but vastly different Sr concentrations, enabling a distinction to be made between end-members, (2) no correlation exists between $^{87}\text{Sr}/^{86}\text{Sr}$ ratios and Sr concentrations of the pre-cleaned cotton residues, ruling out the possibility that archaeological $^{87}\text{Sr}/^{86}\text{Sr}$ ratios have been systematically altered towards the ratios of local sand contaminants and (3) the material existed in an arid environment, never having been waterlogged. Although the additional information provided by the concentration data does not strictly define the availability of Sr in each endmember pool, it can be used to provide a quantitative estimation of the amount of contaminant Sr being removed.

Sample I.D.	Lab I.D.	Type	Taxa	¹⁴ C Age (BP)	Error	Calibrated range 2 sigmas (95.4 %)
60700	SacA 31286 (Lyon-9756)	Charred seed	<i>Gossypium sp.</i>	1690	30	255 - 423 CE
80106	SacA 31285 (Lyon-9755)	Charred seed	<i>Gossypium sp.</i>	1850	30	120 - 306 CE
80124	SacA 31284 (Lyon-9754)	Charred seed	<i>Gossypium sp.</i>	1815	30	130 - 330 CE
80166	SacA 31283 (Lyon-9753)	Charred seed	<i>Gossypium sp.</i>	1725	30	249 - 409 CE
50432_T32	ECHo1839 (Muse 17298)	Desiccated textile	<i>Gossypium sp.</i>	2000	25	47 BCE- 76 CE
50432_T41	ECHo1840 (Muse 17299)	Desiccated textile	<i>Gossypium sp.</i>	1860	25	126 - 236 CE
60628	ECHo 4540 (Muse 21122)	Charred seed	<i>Phoenix dactylifera</i>	1 630	25	402-540 CE
25017	ECHo 4521 (Muse 21123)	Charred seed	<i>Hordeum vulgare</i>	1 890	25	80-225 CE
80022	ECHo 4522 (Muse 21124)	Charred seed	<i>Phoenix dactylifera</i>	1 890	25	80-225 CE
60641	ECHo 4523 (Muse 21125)	Charred seed	<i>Gossypium sp.</i>	1 820	25	131-325 CE
10061	SacA 18212 (Lyon-6669)	Wood charcoal	Unknown	1 875	30	83-237 CE
20026	SacA 18214 (Lyon-6671)	Wood charcoal	Unknown	1850	30	120-306 CE
DDN_E_39 (1)	ECHo 4798 (Muse 22036)	Charred seed	<i>Gossypium sp.</i>	1585	25	423-547 CE
DDN_E_39 (2)	ECHo 4799 (Muse 22037)	Charred seed	<i>Gossypium sp.</i>	1610	25	415-540 CE

Table S5. Radiocarbon dates of archaeological layers containing cotton from Hegra and Dadan, either directly on cotton seeds and textiles or indirectly when cotton was not present in enough quantity. The radiocarbon ages are calibrated using the Oxcal 4.4. software and the IntCal20 atmospheric curve (Bronk Ramsey, 2020; Reimer et al., 2020).

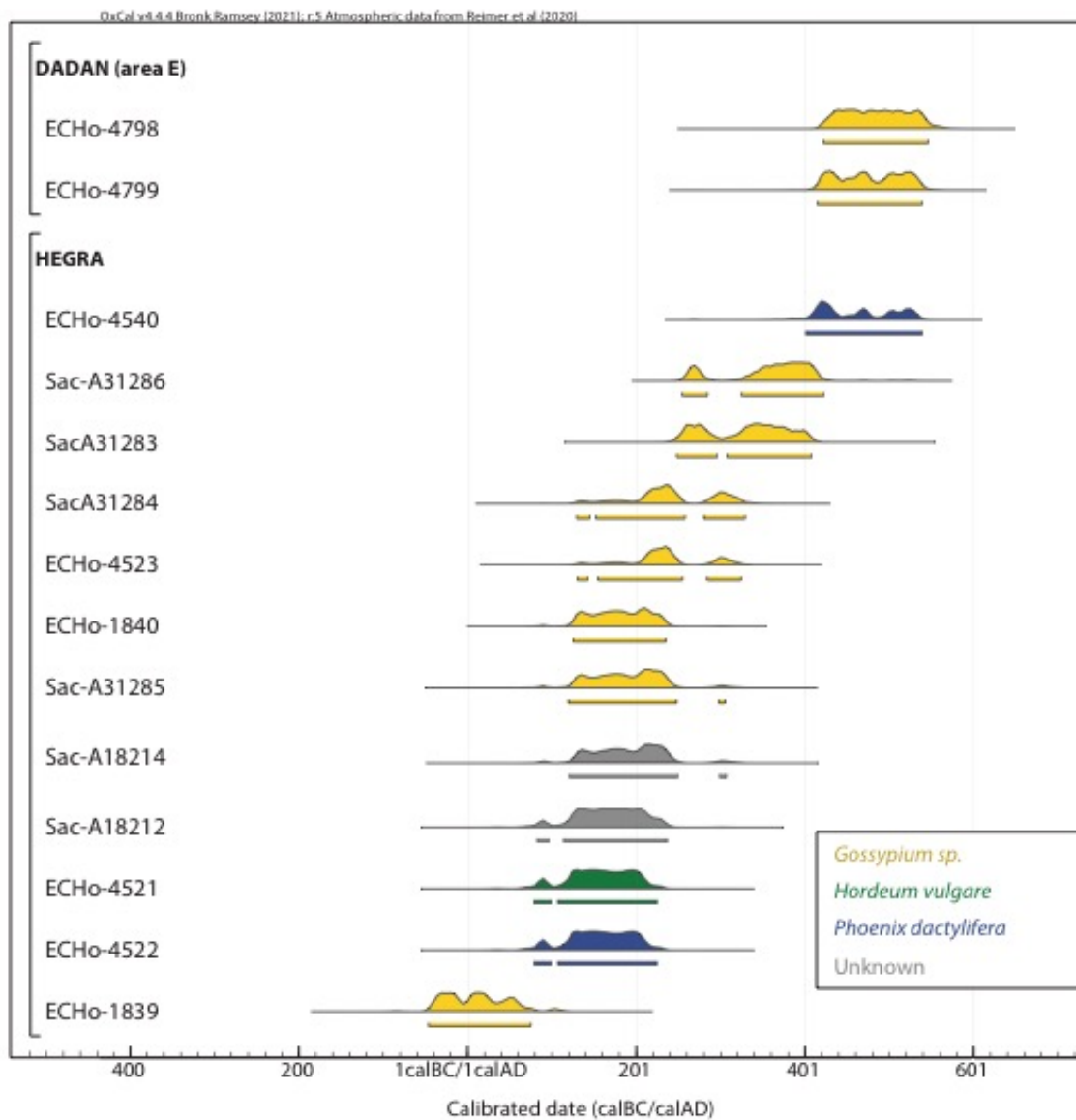


Figure S12. Radiocarbon dates of seeds and textiles from Hegra and Dadan. The radiocarbon ages are calibrated using the Oxcal 4.4. software and the IntCal20 atmospheric curve (Bronk Ramsey, 2020; Reimer et al., 2020).

SI References

- Bogaard, A., Henton, E., Evans, J.A., Twiss, K.C., Charles, M.P., Vaiglova, P., Russell, N., 2014. Locating land use at Neolithic Çatalhöyük, Turkey: The implications of $^{87}\text{Sr}/^{86}\text{Sr}$ signatures in plants and sheep tooth sequences. *Archaeometry*. doi:10.1111/arcm.12049
- Bouchaud, C., 2015. Agrarian Legacies and Innovations in the Nabataean Territory. *Archeosciences, Rev. d'Archéométrie*, G.M.P.C.A./Presses Univ. Rennes 39, 103–124.
- Bouchaud, C., Sachet, I., Dal Prà, P., Delhopital, N., Douaud, R., Leguilloux, M., 2015. New discoveries in a Nabataean tomb. Burial practices and “plant jewellery” in ancient Hegra (Madâ'in Sâlih, Saudi Arabia). *Arab. Archaeol. Epigr.* 26. doi:10.1111/aae.12047
- Bouchaud, C., Tengberg, M., Prà, P.D., 2011. Cotton cultivation and textile production in the Arabian Peninsula during antiquity; the evidence from Madâ'in Sâlih (Saudi Arabia) and Qal'at al-Bahrain (Bahrain). *Veg. Hist. Archaeobot.* doi:10.1007/s00334-011-0296-0
- Brown, G.F., Schmidt, D.L., Huffman, A.C., 1989. *Geology of the Arabian Peninsula. Shield Area of Western Saudi Arabia* US Geological Survey Professional Paper 560–A.
- Camp, V.E., Roobol, M.J., 1992. Upwelling asthenosphere beneath western Arabia and its regional implications. *J. Geophys. Res.* 97. doi:10.1029/92jb00943
- Cequier-Sánchez, E., Rodríguez, C., Ravelo, Á.G., Zárate, R., 2008. Dichloromethane as a solvent for lipid extraction and assessment of lipid classes and fatty acids from samples of different natures. *J. Agric. Food Chem.* 56. doi:10.1021/jf073471e
- Coleman, R.G., 1993. *Geologic Evolution of the Red Sea*. Oxford Monographs on Geology and Geophysics vol. 24. Oxford University Press, Oxford.
- Coleman, R.G., Gregory, R.T., Brown, G.F., 1983. *Cenozoic volcanic rocks of Saudi Arabia*.
- Frei, K.M., Bjerregaard, L., 2017. Provenance investigations of raw materials in pre-Columbian textiles from Pachacamac; strontium isotope analyses, in: Peters, L.B. and A. (Ed.), *PreColumbian Textile Conference VII / Jornadas de Textiles PreColombinos VII*. Zea Books, Lincoln, NE, pp. 387–397. doi:10.13014/K25D8Q1X
- Frei, K.M., Frei, R., Mannering, U., Gleba, M., Nosch, M.L., Lyngstrøm, H., 2009. Provenance of Ancient Textiles—a Pilot Study Evaluating the Strontium Isotope System in Wool. *Archaeometry* 51, 252–276. doi:10.1111/j.1475-4754.2008.00396.x
- Heier, A., Evans, J.A., Montgomery, J., 2009. The potential of carbonized grain to preserve biogenic $^{87}\text{Sr}/^{86}\text{Sr}$ signatures within the burial environment. *Archaeometry*. doi:10.1111/j.1475-4754.2008.00409.x
- Larsson, M., Magnell, O., Styring, A., Lagerås, P., Evans, J., 2020. Movement of agricultural products in the Scandinavian Iron Age during the first millennium AD: $^{87}\text{Sr}/^{86}\text{Sr}$ values of archaeological crops and animals in southern Sweden. *Sci. Technol. Archaeol. Res.* 6, 96–112. doi:10.1080/20548923.2020.1840121
- Macdonald, M.C.A., 1997. Trade routes and trade goods at the northern end of the ‘Incense Road’ in the first millennium BC, in: Avanzini, A. (Ed.), *Profumi d'Arabia: Atti Del Convegno. L'Erma Di Bretschneider*. Rome, pp. 333–50.
- Nehmé, L., 2021. *Guide to Hegra. Archaeology in the Land of the Nabataeans of Arabia*. SKIRA.
- Rohmer, J., Lesguer, F., Bouchaud, C., Purdue, L., Alsuhaibani, A., Tourtet, F., Monchot, H., Dabrowski, V., Decaix, A., Desormeau, X., 2022. New clues to the development of the oasis of Dadan. Results from a test excavation at Tall al-Sâlimiyyah (al-'Ulâ, Saudi Arabia), in: Foote, R., Guagnin, M., Périssé, I., Karacic, S. (Eds.), *Revealing Cultural Landscapes in Northwest Arabia. Papers from the Special Session of the Seminar for Arabian Studies*. Archaeopress, Oxford, pp. 155–188.
- Ryan, S.E., Dabrowski, V., Dapoigny, A., Gauthier, C., Douville, E., Tengberg, M., Kerfant, C., Mouton, M., Desormeau, X., Noûs, C., Zazzo, A., Bouchaud, C., 2021. Strontium isotope evidence for a trade network between southeastern Arabia and India during Antiquity. *Sci. Rep.* 1–10.
- Styring, A.K., Evans, J.A., Nitsch, E.K., Lee-Thorp, J.A., Bogaard, A., 2019. Revisiting the potential of carbonized grain to preserve biogenic $^{87}\text{Sr}/^{86}\text{Sr}$ signatures within the burial environment. *Archaeometry* 61, 179–193. doi:10.1111/arcm.12398